APTAMER MEDIATED CYTOTOXICITY OF DRUG CARRYING SILICA NANOPARTICLES

by

Göktuğ Karabıyık

Submitted to Graduate School of Natural and Applied Sciences
in Partial Fulfillment of the Requirements
for the Degree of Master of Science in
Biotechnology

Yeditepe University
2018

APTAMER MEDIATED CYTOTOXICITY OF DRUG CARRYING SILICA NANOPARTICLES

APPROVED BY:

Assist. Prof. Dr. Bilge Güvenç Tuna ..... 
(Thesis Supervisor)

Assoc. Prof. Dr. Soner Doğan ..... 
(Thesis Co-supervisor)

Prof. Dr. Veli Cengiz Özalp ..... 

Assoc. Prof. Dr. Banu Mansuroğlu ..... 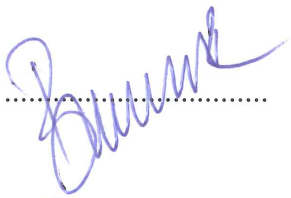

Assist. Prof. Dr. Gülengül Duman ..... 

DATE OF APPROVAL: .... /..../2018

ACKNOWLEDGEMENTS

I would like to thank my MSc supervisors Asst. Prof. Bilge Güvenç TUNA and Assoc. Prof. Soner DOĞAN for their continuous support and motivation during my MSc study. In addition to taking part in this research, working with their research groups provided me invaluable experiences and courage to work harder for further achievements.

I would like to specially thank Assoc. Prof. Veli Cengiz ÖZALP and MSc. Samet UÇAK for their contributions on synthesis and characterization of drug delivery system used in this research and their support during research. For the use of the facilities, I would like to thank the Konya Food and Agriculture University, Research and Development Center for Diagnostic Kits (KITARGEM).

Also, I sincerely thank to my lab mates, Burcu Çiçekdal, Ümit Özorhan, Cihan Erdoğan, Batuhan Mert Kalkan, Nazlı Ataş, and interns worked with our research group during this time for their help, support, and endless cheerfulness.

Finally, I would like to thank my family for their lifetime support.

ABSTRACT

APTAMER MEDIATED CYTOTOXICITY OF DRUG CARRYING SILICA NANOPARTICLES

Aptamers are single stranded DNA or RNA molecules which have high affinity and specificity against their targets. Aptamer AS1411 targets nucleolin protein which is upregulated on cell surface of variety of cancer types. AS1411 aptamer capped MCM-41 mesoporous silica nanoparticles can be utilized as a targeted drug delivery system. This study aims to assess the targeting ability, localization, and cytotoxicity of drug loaded AS1411 aptamer capped MCM-41 type silica nanoparticles (Apta-NP) on nucleolin positive triple negative murine breast cancer cells, E0771. Capping of mesoporous silica nanoparticles with AS1411 aptamer inhibits drug release from pores of nanoparticle in closed conformation, when AS1411 aptamer interacts with its target, nucleolin, conformational change on aptamer structure induces drug release. In this study, in order to show cellular localization and uptake of Apta-NP drug delivery system, first, E0771 cells were treated with either fluorescein loaded Apta-NP (Apta-NP-Fl) delivery system or fluorescein loaded NP (NP-Fl). Increased uptake of fluorescein was measured in cells treated with Apta-NP-Fl in comparison to NP-Fl. Later, the same cell line was incubated with either paclitaxel loaded Apta-NP (Apta-NP-TXL) or free paclitaxel in range of 0-100 µM for 24 or 48 hours and cell viability was measured. IC50 values for free TXL and Apta-NP-TXL delivery system were 45.76 µM and 36.41 µM, respectively after 24 hours incubation while values were 48.87 µM and 35.64 µM after 48 hours incubation. Then, to examine in vivo targeting ability of Ap-NP system, E0771 cells were inoculated into right flank of C57bl/6 mice and localization of fluorescein cargo of Apta-NP delivery system was determined using in vivo fluorescence imaging technique. One hour after the injection, localization of fluorescence signal around tumor region was observed. 24 hours after injection, fluorescence signal was cleared off the body. Therefore, Apta-NP complex might be suggested as a good candidate for targeted breast cancer therapy in respect to lower IC50 value on murine breast cancer cell line and ability to localize on allograft breast cancer model.

ÖZET

İLAÇ TAŞIYAN SİLİKA NANOPARTİKÜLLERİN APTAMER ARACILIĞIYLA OLUŞTURDUĞU SİTOTOKSİSİTE

Aptamerler, hedeflerine yüksek afinite ve spesifite gösteren, tek zincirli DNA ya da RNA moleküleridir. AS1411 aptamer, özellikle birçok kanser tipi hücrelerinin hücre zarında yüksek miktarda görülen nükleolin proteinini hedefler. AS1411 aptameri MCM-41 tipi mezoporlu silika nanokürelerine konjüge edilerek, hedefli ilaç taşıma sistemi olarak kullanılabilir. Bu amacı, ilaç enkapsüle edilmiş AS1411 konjüge edilmiş MCM-41 tipi silika nanokürelerinin (Apta-NP), nükleolin pozitif triple negatif rodent meme kanseri hücre hattında (E0771) hedefleme yeteneğini, lokalizasyonunu ve sadece kanser ilacı kullanımına oranla sitotoksisitesini göstermektir. AS1411 aptamerinin mezoporlu silika nanokürelere konjügasyonu nanokürelerden ilaç salınımı durdurmaktadır. Aptamer nükleolin proteini ile etkileşime girdiğinde mezopor açılır ve ilaç salınımı gerçekleşir. Bu çalışmada taşıma sisteminin hücrede lokalizasyon ve hedefleme yeteneğini ölçmek amacı ile E0771 hücre hattı öncelikle, floresan yüklü Apta-NP taşıma sistemi veya floresan yüklü NP ile muamele edildi. Sadece floresan grubuna göre, floresan boyalı hücre miktarında artış gözlemlendi. Apta-NP taşıma sisteminin, sadece ilaç muamelesine göre artması beklenen sitotoksisitesini göstermek amacı ile, hücreler eşit miktarda (0-100μM) paclitaxel taşıyan, Apta-NP taşıma sistemi veya sadece paclitaxel ile 24 veya 48 saat muamele edildiler ve WST-1 metodu kullanılarak, ilaçların sitotoksik etkileri karşılaştırıldı. Sadece ilaç kullanımı veya paclitaxel taşıyan, Apta-NP taşıma sistemi kullanımı sonucunda hesaplanan IC50 değerleri, 24 saat için sırasıyla, 45.76 μM and 36.41 μM, 48 saat için sırasıyla 48.87 μM and 35.64 μM dır. Bu çalışmaları takiben, allograft meme kanseri modeli C57bl/6 farelerinde, sağ flank bölgesine E0771 hücre inokülasyonu ile oluşturuldu. Apta-NP taşıma sisteminin lokalizasyonu, in vivo floresan görüntüleme metoduyla gözlendi. Enjeksiyondan bir saat sonra, meme tümörü çevresinde floresan lokalizasyonu gözükmeye başlarken, enjeksiyondan 24 saat sonrasında, floresanın vücuttan atılmış olduğu gözlemlendi. Sonuç olarak, IC50 değerinin daha düşük olması ve in vivo lokalizasyonunun sağlanabilmesine dayanarak, Apta-NP taşıma sistemi, hedefli meme kanseri tedavisi için umut vadettiğini önerilebilir.

TABLE OF CONTENTS

ACKNOWLEDGEMENTS iii

ABSTRACT iv

ÖZET v

LIST OF FIGURES viii

LIST OF TABLES ix

LIST OF SYMBOLS/ABBREVIATIONS x

1. INTRODUCTION 1

1.1. AIM OF THE STUDY 1

1.2. BREAST CANCER 1

1.3. BREAST CANCER THERAPY 3

1.3.1. Current Chemotherapeutic Agents Used in Clinics 4

1.3.1.1. Paclitaxel (Taxol®) 4

1.3.1.2. Doxorubicin 5

1.4. TARGETED DELIVERY FOR BREAST CANCER THERAPY 6

1.4.1. Monoclonal Antibodies 7

1.4.2. Aptamers 7

1.4.2.1. Systemic Evolution of Ligands by Exponential Enrichment (SELEX) 9

1.4.3. Comparison of Aptamers and Monoclonal Antibodies 10

1.5. APTAMER-NANOPARTICLE COMPLEX (Apta-NP) 11

1.5.1. AS1411 Aptamer 12

1.5.2. Controlled Release 14

2. MATERIALS AND METHODS 19

2.1. MATERIALS 19

2.1.1. Consumables 19

2.1.2. Chemicals 19

2.1.3. Instruments 20

2.1.4. Cell Line 20

2.2. STUDY DESIGN 20

2.3. CELL MAINTENANCE 21

2.4. CHARACTERIZATION OF APTA-NP DRUG DELIVERY SYSTEM 22
2.4.1. TEM Analysis 22
2.4.2. SEM Analysis 22
2.4.3. AFM Analysis 22
2.4.4. DLS Analysis 23
2.4.5. FTIR Analysis 23
2.4.6. Measurement of Cellular Uptake of Apta-NP-Fl by Flow Cytometry 23
2.4.7. Determination of In Vitro Localization and Targeting Ability of Apta-NP System by Fluorescence Microscopy 23
2.5. MEASUREMENT OF CYTOTOXICITY of APTA-NP-TXL ON BREAST CANCER CELLS 24
2.6. IN VIVO EXPERIMENTS 25
2.6.1. Animals 25
2.6.2. Allograft Tumor Model 25
2.6.3. In Vivo Imaging 25
2.7. STATISTICAL ANALYSIS 26
3. RESULTS 27
3.1. CHARACTERIZATION OF APTA-NP DRUG DELIVERY SYSTEM 27
3.1.1. In Vitro Uptake 30
3.1.2. In Vitro Localization 32
3.1.3. Measurement of Drug Release from Apta-NP-TXL Drug Delivery System. 34
3.1.4. Cytotoxicity of MCM-41 Type Silica Nanoparticles 35
3.1.5. Cytotoxicity of Paclitaxel Loaded Aptamer-Nanoparticle Complex 36
3.2. IN VIVO EXPERIMENTS 37
3.2.1. In Vivo Localization 37
4. DISCUSSION 39
5. CONCLUSION 42
6. FUTURE DIRECTIONS 43
REFERENCES 44
APPENDIX A 70

LIST OF FIGURES

Figure 1.1. AS1411 conjugated Paclitaxel loaded MCM-41 nanoparticle complex 11

Figure 1.2. AS1411 mechanism of action..... 14

Figure 1.3. Controlled release strategies for silica nanoparticles 16

Figure 3.1. TEM images MCM-41 type mesoporous silica nanoparticles 27

Figure 3.2. SEM images of MCM-41 type mesoporous silica nanoparticles 28

Figure 3.3. Nanometric imaging of MCM-41 type mesoporous silica nanoparticles..... 29

Figure 3.4. Average diameter of MCM-41 type mesoporous silica nanoparticles 29

Figure 3.5. FTIR spectra of MCM-41 type mesoporous silica nanoparticles..... 30

Figure 3.6. Representative dot plots of fluorescein uptake of E0771 cells 31

Figure 3.7. Quantification of in vitro fluorescence uptake of E0771 cells 32

Figure 3.8. In vitro uptake and localization of Fluorescein 33

Figure 3.9. Time dependent drug release from Apta-NP-TXL complex 34

Figure 3.10. Effect of MCM-41 type NP exposure on cell viability. 35

Figure 3.11. Effect of Apta-NP -TXL exposure on cell viability 36

Figure 3.12. In vivo Localization of Apta-NP complex around tumor region. 38

LIST OF TABLES

Table 1.1. Molecular subtypes of breast cancer and incidence in Turkey 3

Table 2.1. Consumables used for cell culture experiments 19

Table 2.2. Chemicals used for cell culture experiments 19

Table 2.3. Instruments used in experiments 20

Table 3.1. Comparison of IC50 values for Apta-NP-TXL or free TXL treatment 37

LIST OF SYMBOLS/ABBREVIATIONS

°C	Degree centigrade
µg/ml	Microgram per milliliter
µM	Micromolar
ABCB1	ATP-binding cassette sub-family B member 1
ABCC1	ATP-binding cassette sub-family C member 1
AFM	Atomic force microscopy
AIDS	Acquired immune deficiency syndrome
AJCC	The American Joint Committee on Cancer
AMD	Age related macular degeneration
ANOVA	Analysis of variance
Apta-NP	Aptamer conjugated silica nanoparticle
Apta-NP-Fl	Fluorescein loaded aptamer conjugated silica nanoparticle
Apta-NP-TXL	Paclitaxel loaded aptamer conjugated silica nanoparticle
bcl-2	B-cell lymphoma 2
CaCl2	Calcium chloride
CO2	Carbon dioxide
CXCL-12	C-X-C motif chemokine ligand 12
DAPI	4′,6-diamidino-2-phenylindole
DLS	Dynamic light scattering
DMSO	Dimethyl sulfoxide
EpCAM	Epithelial cell adhesion molecule
FAM	Fluorescein
FBS	Fetal bovine serum
FDA	Federal Drug Agency
FTIR	Fourier-Transform infrared spectroscopy
g	Gravitational force
GFP	Green fluorescein protein
GRO	G-rich oligonucleotides
h	Hour

HER-2	Human epidermal growth factor receptor-2
HIV	Human immunodeficiency virus
IC50	Half maximal inhibitory concentration
IKK	I kappa B kinase
kDa	Kilodalton
M	Molarity
MCM-41	Mobile crystalline material type 41
n	Sample size
NCI	National Cancer Institute
NF- κB	Nuclear factor kappa-light-chain-enhancer of activated B cells
NP	Silica nanoparticle
NP-Fl	Fluorescein loaded silica nanoparticle
NSCLC	Non-small cell lung cancer
PBS	Phosphate buffered saline
PCR	Polymerase chain reaction
PEG	Polyethylene glycol
Pen/Strep	Penicillin/Streptomycin
PFA	Paraformaldehyde
RPMI 1640	Roswell Park Memorial Institute medium
SD	Standard deviation
SELEX	Systematic evolution of ligands by exponential enrichment
SEM	Scanning electron microscopy
TEM	Transmission electron microscopy
TXL	Paclitaxel
UV	Ultraviolet
VEGF	Vascular endothelial growth factor
VWF	Von Willebrand factor
YÜDETAM	Yeditepe Üniversitesi Tıp Fakültesi Deneysel Araştırmalar Merkezi

1. INTRODUCTION

1.1. AIM OF THE STUDY

Aim of this study is to assess the localization, uptake, and cytotoxicity of Apta-NP drug delivery system on in vitro and in vivo breast cancer models.

For that purpose, in this study, we used paclitaxel as chemotherapeutic agent, then loaded it within MCM-41 mesoporous silica nanoparticles. As targeting agent, nucleolin targeting aptamer AS1411 have been used to cap pores on MCM-41 silica nanoparticles which also provided controlled release by using aptamer as nanovalve on the drug delivery system. By using this drug delivery system, we assessed the effect of aptamer mediated silica nanoparticle usage on efficiency of drug delivery and cytotoxic effect in comparison to free paclitaxel.

1.2. BREAST CANCER

Dramatic increase on the incidence of breast cancer has been reported for both Turkish population and world population in general [1, 2]. According to reports, breast cancer incidence in Turkey was 25 per 100 thousand people in 1993 while the incidence was doubled 20 years later and reported as 50 per 100 thousand people. However, the data obtained may be less than the real prevalence due to lack of cancer screening system and different risk factors on eastern and western provinces of Turkey [1, 3]. In addition to the fact that breast cancer is the most common cancer type for Turkish women, higher incidence and poorer prognosis was observed on medical cases in Turkey in comparison to developed countries [4]. Furthermore, age adjusted breast cancer related mortality rate has been reported as 11.9 per 100 thousand women [5].

As reported by GLOBOCAN project 2012, situation is similar for the world population. Estimated breast cancer incidence is 17 per 100 thousand women, covering 30.2 per cent of all estimated new cancer cases. Furthermore, number of new cases and number breast cancer related death are expected to increase year by year [6, 7]. In addition to new cases, estimated

breast cancer related mortality rate is 4.4 per 100 thousand people per year for women covering 25.1 per cent of all estimated cancer related mortality [2]. Even though total mortality rate of breast cancer rate for women decreases year by year in US population [8], number of estimated new cases and number of death related to breast cancer increases year by year [6, 7].

Breast tumors are categorized into histological and molecular subtypes to define prognosis and therapeutic methods of the disease [9]. Histological grades determine differentiation level of breast cancer cells from normal breast cells. In this grading system, Grade I refers to breast cancer cells which grow slowly, and those cells are morphologically similar to normal breast cells. Grade III breast cancer cells grow and divide rapidly, and they are morphologically different than normal breast cells [10-12]. A study conducted in Turkey, including 13,240 breast cancer patients, reports that 50 per cent of patients have been diagnosed with histological Grade III [4]. Histological tumor stages are determined by TNM categorization method developed by American Joint Committee on Cancer (AJCC) which considers tumor size (T), node status (N) and metastasis (M). By this method, breast tumors are divided to stages. Lowest stage is Stage 0 which includes breast tumors with non-invasive abnormal cells and no node or distant metastasis while highest stage is Stage IV which includes breast tumors with distant metastasis. Histological stages define the extent of breast cancer [11, 13]. 44 for per cent of patients in the study stated above have been diagnosed with Stage II [4].

Molecular subtypes of breast cancer are divided into five groups depending on their hormone receptor expression on cell surface such as Luminal A-like, Luminal B/HER2 negative-like, Luminal B/HER2 positive-like, HER2-type and Triple Negative [14-17]. Presence or absence of those hormone receptors determine the prognosis of the disease and therapeutic options [18, 19]. 62 per cent of patients in the study stated above have been diagnosed with Luminal A-like breast cancer [4].

Table 1.1. Molecular subtypes of breast cancer and incidence in Turkey [4, 17]

Molecular Subtype	ER and/or PR	HER2 receptor	Incidence in Turkey
Luminal A-like	+	-	62%
Luminal B/HER2-	+	-	15%
Luminal B/HER2+	+	+	
HER2-type	-	+	8.50%
Triple Negative	-	-	15%

1.3. BREAST CANCER THERAPY

Therapeutic options for breast cancer therapy differ in respect to the histological and molecular subtype of the disease. As the disease progresses, therapeutic efficacy decreases. Hormone receptor positive subtypes of breast cancer are more common and better prognosis is expected because of availability of targeting drugs used in clinics. Hormone therapy or receptor targeting drugs like trastuzumab which targets HER-2 receptor, can be used for those patients with hormone receptor positive breast tumors. However, hormone receptor negative subtypes show poor prognosis due to lack of targeting drugs and extent of the disease [17, 20, 21]. Radiotherapy or other chemotherapeutic drugs like doxorubicin should be used in addition to surgical therapy for hormone receptor negative breast tumors. [17, 22]. Furthermore, patients with higher histological tumor grades have significantly increased recurrence rates, even with a successful surgical therapy [23, 24]. Moreover, some patients develop resistance to chemotherapeutic drugs such as doxorubicin. There are severe side effects of chemotherapeutic drugs such as cardiotoxicity, hypersensitivity and peripheral neuropathy. Because of those reason advanced methods which combine multiple agents must be developed and used in clinics [25]. Early prognosis or prevention of breast cancer would be the best outcome for future studies [26]. However, as stated above, number of patients with breast cancer increases day by day. Current therapeutic approaches, as they will be explained below, are not sufficient enough for breast cancer therapy and more efficient tools for patients with poor breast cancer prognosis are required. For this purpose, efficiency of a novel drug delivery system which delivers chemotherapeutic agent to the cancer tissue selectively and controls pharmacodynamic properties of chemotherapeutic agent actively by using nucleolin targeting aptamer gated drug delivery system has been researched in this study.

1.3.1. Current Chemotherapeutic Agents Used in Clinics

1.3.1.1. Paclitaxel (Taxol®)

Taxol® is a product of the antitumor agent screening conducted by National Cancer Institute (NCI) initiated in 1960. Active compound, paclitaxel, was extracted from western yew, *Taxus Brevifolia*, showed toxicity against rodent tumors and cancer cell lines [27]. Studies showed that cytotoxic effect of Paclitaxel is caused by stabilization of microtubules when cells are exposed to drug [28, 29]. Microtubules are one of the major classes of cytoskeleton proteins which take part in many cellular functions including migration, cilia and flagella formation and chromosome segregation during mitosis. Homologous α and β tubulin proteins are subunits of microtubules. As concentration of α-β tubulin passes critical concentration, polymerization event starts. Polymerization is temperature and concentration dependent and depending on the cellular event, microtubules are polymerized or depolymerized constantly [30-32]. Paclitaxel decrease critical concentration for polymerization and stabilizes formed microtubules structures. Thus, cells cannot execute cellular process like migration and division which require microtubule polymerization and depolymerization [28, 29]. Anti-proliferative effect of Paclitaxel® has been shown on many cancer cell lines including HeLa cells [33]. Normally, microtubules destabilize when cells are treated with $CaCl_2$ or incubated at +4°C. Paclitaxel exposure can stabilize microtubules even under physiological destabilization conditions as stated above. To test efficiency of Paclitaxel under those conditions HeLa cells have been treated with Paclitaxel® and microtubule structures stayed stable under those conditions [34]. Also in mouse fibroblast cells similar effects have been shown [33]. Paclitaxel has been approved by FDA in 1994 for breast carcinoma [27], and still is being used for breast cancer therapy [35].

Similar to other anticancer agents, paclitaxel has side effects due to its cytotoxic nature [36]. Peripheral neuropathy, disorders in peripheral nervous system, has been diagnosed in dose dependent manner on patients taking paclitaxel as medication. That is the main side effect which prevents application of drugs with higher dosage [37]. Decreasing concentration of drug also decreases therapeutic efficacy. In addition to peripheral neuropathy, cardiotoxicity on older women with metastatic breast cancer [38], hypersensitivity [39], hematologic toxicities like, neutropenia [39], infections like neutropenic enterocolitis [40] and muscle

pain [41] have been reported for patients using paclitaxel. Novel delivery strategies like stimuli-dependent controlled release of drug to targeted tissue would decrease side effects and toxicity of Paclitaxel administration [42].

Moreover, studies showed that, paclitaxel's half-life is around two hours for different types of solid tumors including breast, lung, ovarian cancers [43, 44]. To overcome short half-life of paclitaxel, methods such as combination therapy have been used. In their study, Qi et al showed that, using VEGF inhibitor, monoclonal antibody drug, Avastin in addition to paclitaxel for non-small cell lung cancer (NSCLC) expands the duration of paclitaxel exposure around tumor tissue. They hypothesize that this effect is due to combination of inhibition of angiogenesis around tumor tissue, and therapeutic effect of Avastin. Also, as we used in this study, nanoparticle-based drug delivery systems also increase half-life of the drug in circulation [45, 46]

1.3.1.2. Doxorubicin

Doxorubicin is a chemotherapeutic agent in the class of anthracyclines. Doxorubicin firstly extracted from *Streptomyces* bacteria as a cytotoxic agent [47]. Doxorubicin has two different mechanisms of actions as a chemotherapeutic agent. Firstly, doxorubicin inhibits topoisomerase-II mediated DNA repair by interacting tightly with minor groove of DNA [48]. Topoisomerase-II takes part in releasing the tension on DNA strands which formed during events like transcription and other DNA related cellular processes [49]. Inhibition of topoisomerase-II activity causes DNA damage and cell death [48]. Secondly, doxorubicin increases oxidative stress within cell by disrupting redox balance and generating reactive oxygen species [50-52].

Doxorubicin has been approved by FDA for metastatic breast cancer therapy in 1974 and since then it has been used in clinics [53]. however, doxorubicin has also limitations as a therapeutic agent for breast cancer therapy. Firstly, doxorubicin resistance is an important factor which limits efficacy of the drug [54]. Enhanced expression of efflux pumps like ABCB1, ABCC1 decreases intracellular concentration of drug [55, 56] in which drug is pumped out of the cell continuously and therapeutic effect decreases [57].

Furthermore, cardiotoxicity like side effects are some of the limiting factors for doxorubicin treatment in addition to drug resistance [54, 55]. Studies shown that, around two to five per cent of patients taking doxorubicin as medication, shown evidence for congestive heart failure or significant decline on left ventricular function which occurs due to effect of doxorubicin on disruption of redox balance within myocardial cells [58-61]. With targeted delivery, accumulation of doxorubicin on cardiac tissue can be decreased and more efficient therapy can be facilitated via controlled release of drug around tumor tissue. Despite many targeted delivery and controlled release systems were suggested previously, still more effective, novel methods are demanded.

1.4. TARGETED DELIVERY FOR BREAST CANCER THERAPY

Paul Ehrlich, a Nobel laureate immunologist, provided the idea of *"Magische Kugel"*, magic bullet in English, as the definition of ideal drug in early 1900's which targets only certain disease-making-pathogens. His idea was that an ideal drug, should be able to target only the cause of the disease and effected cells in the body and should not be harmful to the healthy cells of the patient. Currently, drugs being used in clinics like Paclitaxel and doxorubicin, for breast cancer chemotherapy have side effects due to their inability to differentiate healthy dividing cells from cancer cells as stated above. Toxicity of those drugs on healthy cells is one of the dose-limiting factors which decrease efficacy of the drug [62, 63]. Because of that reason, targeted therapy is a popular method among scientists working on breast cancer therapeutics. Targeted therapy aims to provide highest concentration of drug to tumor microenvironment without harming healthy cells [64]. With targeted therapy, in addition to decreasing side effects of the drugs, problems like resistance against chemotherapeutic agent can be solved [64]. Protein based monoclonal antibodies and single stranded oligonucleotide-based aptamers are some of the most promising agents to be used in targeted therapy against breast cancer [64-66]. Moreover, those agents can also be used for cancer diagnosis due to their ability to locate their target in vivo [67, 68].

1.4.1. Monoclonal Antibodies

Ehrlich's magic bullet idea substantiated in second half of the 20th century by production of monoclonal antibodies. In 1975, Georges Kohler and Cesar Milstein produced monoclonal antibodies by using hybridoma technique in which mouse myeloma and mouse spleen cells are fused and monoclonal antibodies are procured from those cells [69].

Monoclonal antibodies are immunoglobin shaped proteins which are produced by immune cells originated from single parent cell, against certain targets. Their size is around 150kDa [70]. Monoclonal antibodies recognize certain span of amino acids on their target and their target area is called as epitope. [69, 71, 72]. Due to their ability to target specific "markers", monoclonal antibodies took attention of many researchers as a tool for developing new targeting drugs for many diseases. Currently there are more than fifty monoclonal antibody-based drugs approved by FDA [72, 73].

First monoclonal antibody approved by FDA for breast cancer therapy was trastuzumab, *Herceptin*®. Trastuzumab targets HER-2, a growth factor receptor overexpressed in HER-2 positive breast cancer cells while lowly expressed on healthy cells of the patient [74, 75]. It has been shown that free trastuzumab improves patient outcomes on early breast cancer [75, 76]. However, trastuzumab resistance has been observed in clinical cases. Around 35 per cent of the HER-2 positive breast cancer patients respond free trastuzumab therapy [77, 78]. Moreover, side effects including cardiotoxicity have been observed on patients taking trastuzumab as medication [77, 79]. In addition to its efficacy as a free drug, trastuzumab has been used as a guiding agent for chemotherapeutic drugs loaded by nanoparticles. Even though those methods are not in the clinics yet, higher efficacy of trastuzumab functionalized nanoparticles against breast cancer cells in comparison to free trastuzumab has been reported [80-83].

1.4.2. Aptamers

Aptamers are single stranded DNA or RNA oligonucleotides which have high affinity to their specific targets. In 1990, Tuerk et al reported that, from a population of random sequences, 65,536 different oligonucleotides in their case, a specific RNA ligand with high affinity to a certain protein can be chosen by applying multiple rounds of selection/evolution,

as it is called Systematic Evolution of Ligands by Exponential Enrichment (SELEX) by them [84]. In the same year, Ellington et al reported that, from 10^{13} random RNA sequences, specific RNA oligonucleotides have ability to bind a variety of organic dyes [85]. In the same paper, those specific oligonucleotides have been named as "*aptamers*" from Latin word "*aptus*" in the meaning of -to fit- and from Greek word "*meros*" in the meaning of -part- [85, 86]. Currently there are lots of aptamers being studied. And studies showed that aptamers can target a variety of molecules from ions to cell types [86].

Pegaptanib sodium, *Macugen*®, is the first FDA approved aptamer-drug in 2004 [87, 88], manufactured for the disease age related macular degeneration (AMD). This disease is one of the important reasons for blindness for older individuals [88]. Pegaptanib sodium is a Vascular Endothelial Growth Factor (VEGF) antagonist and it binds to pathological isoform of extracellular VEGF. Interaction of pegaptanib and VEGF inhibits pathological neovascularization [89]. Pegaptanib sodium is currently being used in clinics efficiently as a beneficial and safe drug [90, 91].

Following *Macugen*® there are many aptamer-drug candidates on clinical trials. As a promising antithrombic agent, ARC-1779 aptamer is targeting von Willebrand factor (VWF) is a glycoprotein taking part in thrombosis procedure in which VWF interacts with pro-coagulant factor VIII and mediates platelet adhesion on wound surface [92, 93]. Also, high levels of VWF has been shown on acute coronary syndromes [94], acute myocardial infarction [94] and ischemic stroke [95]. ARC-1779 aptamer completed phase II trials as a promising antithrombotic agent due to ability of ARC-1779 to target and inhibit VWF to interact with pro-coagulant factor VII and reduce platelet adhesion and thrombus growth [96].

Aptamers are promising agents for drug development field for many diseases including cancer and aptamer-drug candidates against known biomarkers for cancer diagnosis and therapy are being developed [97, 98]. One of those aptamer-drug candidates is NOX-A12 which is in phase II clinical trials [99]. NOX-A12 was developed against stromal-cell derived factor-1 (CXCL-12) as a drug for chronic lymphocytic leukemia. CXCL-12 is a chemokine which is secreted by bone marrow stromal cells, for CXCR-4 and CXCR-7 receptors on leukemia cells which are shown to be upregulated in many cancer types [100-102]. Leukemia cells adhere on bone marrow stromal cells and via CXCL-12 signaling they develop resistance to drug induced apoptosis in the protective niche [102, 103]. Even though

chemotherapeutic agents can kill cancer cells in blood via drug induced apoptosis, adhered cancer cells are protected from this effect [104]. By inhibiting CXCL-12, NOX-A12 remobilizes adhered leukemia cells and they are sensitized against drug induced apoptosis [102].

Aptamers are oligonucleotides with a specific three-dimensional shape with high affinity against their targets as stated above. In addition to aptamer-drugs and aptamer-functionalized nanoparticle-based drugs like the delivery complex of this study, aptamers can also be used in various fields such as for diagnosis for diseases and for detection of chemicals [105]. Aptamer for epithelial cell adhesion molecule (EpCAM) [106], DHX9 [107] for colorectal cancer diagnosis, HER-2 [108], nucleolin [109] for breast cancer diagnosis, troponin aptamer for acute myocardial infarction diagnosis[110], immunodeficiency virus (HIV) aptamer for acquired immune deficiency syndrome (AIDS) [111] and many other aptamer candidates are being studied for diagnostic and imaging tools [112-114].

In addition to therapeutics field, aptamers are promising agents due to many benefits provided by nucleotide structure, and they can be used as aptasensors in many fields like food inspection and safety [115, 116] and analyte detection [117, 118]. Chen et al developed aptamer conjugated gold nanoparticle modified glassy electrode to inspect fumonisin B toxin [119] while Mejri-Omrani et al developed aptamer conjugated dendrimer coated gold nanoparticle to inspect Orhradoxin A [120]. Both studies reached detection level around 2-5 10^{-9} M via electrochemical impedance spectroscopy [121].

1.4.2.1. Systemic Evolution of Ligands by Exponential Enrichment (SELEX)

Majority of aptamers are the result of successive SELEX cycles [122]. Since description of first aptamer selections reported by Tuerk et al [84] and Ellington et al [85], SELEX procedure has been modified depending on the outcome expected from resulting aptamer. In general, SELEX requires a random library of aptamer candidates including high number of different oligonucleotides, Ellington et al used 10^{13} candidates in their research in 1990 [85] while some studies use a library containing around 10^{15} candidates with conservative sequences on 3' and 5' terminals of aptamer candidates [122, 123]. For DNA aptamers, firstly target molecules are incubated with aptamer library. Since aptamers have their specific three-dimensional structures on SELEX conditions, some aptamer candidates

interact with target molecules while unbound candidates are washed away. Bound aptamers are amplified by PCR method and then, this procedure is repeated several times. After total 10-15 cycles, a specific aptamer with high affinity to its target can be obtained [122-124]. Even though the SELEX procedure generally follows steps stated above, depending on the requirement of the researcher different methods are developed. To illustrate, negative SELEX recruits an additional step in which a similar molecule to the target molecule is incubated with aptamer library after primary incubation with the target molecule, and aptamer candidates which interact with similar molecule are removed from the pool to increase specificity to the main target [123, 125] while Covalent SELEX recruits functional group modified aptamer candidates in the aptamer library and they can covalently interact with target molecules [125, 126]. One of the limitations of aptamers is the effect of the target environment. Traditional SELEX procedure is performed with purified targets, however in a cell or tissue, environmental conditions like pH, temperature and effect of other molecules in the environment may change [86, 122, 123]. To overcome this problem, CELL-SELEX can be used to select aptamers which are specific to different cell types thereby, aptamer candidates' reaction in live cells can be tested during SELEX [86, 127, 128]. Even more, SELEX can be applied in vivo. In this way, effect of aptamer candidates in even more complicated environment can be seen. Cheng et al used in vivo SELEX to examine aptamers passing through Blood-Brain-Barrier [129].

1.4.3. Comparison of Aptamers and Monoclonal Antibodies

More than fifty monoclonal antibodies are being used as a therapeutic agent which have been approved by FDA [74, 75]. Even though, only one aptamer drug was approved by FDA, several aptamer drug candidates for many diseases including cancer, are in clinical trials [130, 131]. Aptamers have several superior characteristics against monoclonal antibodies. Aptamers are nucleotide-based compounds unlike monoclonal antibodies which are protein-based compounds. Aptamers are 20-25 times smaller than monoclonal antibodies which provides higher tissue penetration and increased ability to target smaller compounds like ions [132, 133]. Due to oligonucleotide structure of aptamers, they are more resistant against changing environmental conditions like pH and temperature. While antibodies denature on extreme conditions, aptamers regain their structure when conditions are reversed [132, 134, 135]. Because of those properties shelf life of aptamers are also higher than monoclonal

antibodies [135]. However, aptamers are sensitive against nucleases due to their nucleotide-based structure. Modifications on backbone of nucleotides or nucleotide modifications on 3' or 5' terminals of aptamers increase aptamers' resistance against nucleases [136]. Moreover, using modified nucleotides during SELEX procedure also overcomes this problem [137]. In addition to those, renal filtration is a problem for aptamers being developed as a potential drug, addition of protective groups such as polyethylene glycol (PEG) on aptamer increases half-life. This strategy can also be used for monoclonal antibodies [136, 137]. In addition to those, due to protein structure of monoclonal antibodies, mild immune response can be seen while aptamers do not show any reported immune response [132].

Current monoclonal antibody production methods require living cells or animals while aptamers can be produced simply by SELEX procedure, and production of a known aptamer requires simple chemical reactions while each batch of monoclonal antibody production shows differences and requires optimization [105, 138]. Those differences also affect the production cost [105]. Theoretically aptamers can be produced against unlimited targets however antibodies require immune response against target protein from the parent cell [105, 139].

1.5. APTAMER-NANOPARTICLE COMPLEX (Apta-NP)

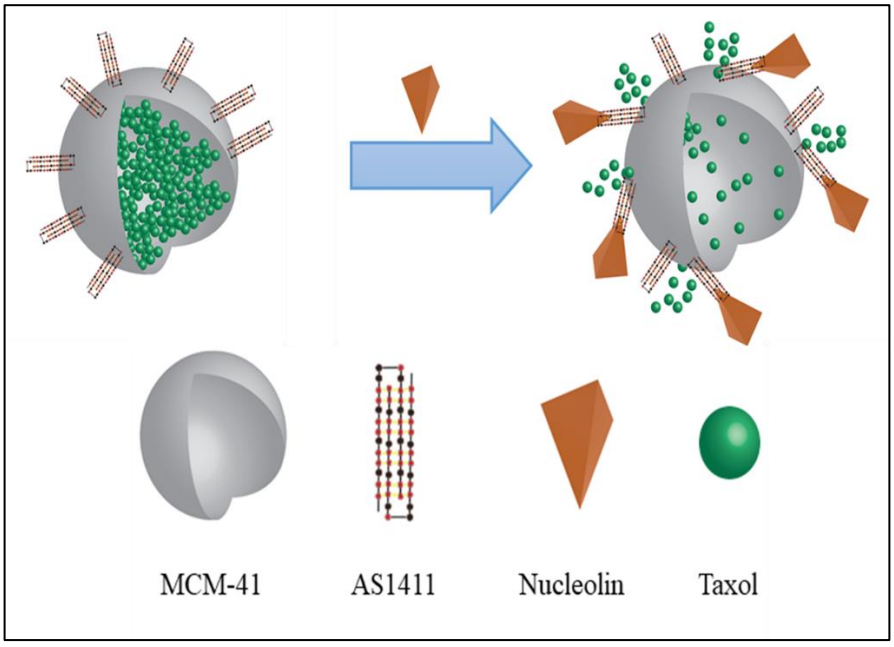

Figure 1.1. AS1411 conjugated Paclitaxel loaded MCM-41 nanoparticle complex

1.5.1. AS1411 Aptamer

G-quadruplex structures are formed by guanine-rich oligonucleotides in which tetrads of guanine bases with hydrogen bonds an example for which can be seen on telomeres [140]. Studies showed that specific topology of g-quadruplex structure, and not anti-sense mechanism due to nucleic acid-based structure, leads new properties like resistance against nucleases, enhanced cellular uptake and most importantly for this study, anti-proliferative effect on cancer cells [141]. Due to those properties of g-quadruplex structures, some researches applied this information to SELEX by alternating nucleotide ratio for the primary library to obtain aptamer candidates with the g-quadruplex properties stated above [142]. Several studies reported that, guanine-rich oligonucleotides exposure to cancer cells suppresses growth and induces apoptosis [141-145].

In their study for cancer specific drug development, Bates et al used different guanine rich phosphodiester oligonucleotides, GRO's as researchers called them [145]. This study revealed that, their candidate GRO's are able to produce antiproliferative effect on breast cancer cell lines due to the specific structure of GRO's and not because of anti-sense mechanism as researchers' primary hypothesis [145]. 26-mer aptamer sequence, 5′-GGTGGTGGTGGTTGTGGTGGTGGTGG named as AGRO100 by researchers, later named as AS1411 by Antisoma, PLC., is a modified product of the research conducted in 1999 unlike other aptamers which are generated by SELEX [146]. Further studies reported that, AS1411 shows a specific anti-proliferative effect against cancer cell lines while on non-malignant cells this effect could not be detected [146, 147]. Following those, it has been identified that, aptamer AS1411 targets nucleolin protein [145, 148, 149]

Nucleolin is a conserved protein forming around 10 per cent of proteins found in nucleolus which suggests that nucleolin takes part in early ribosome biogenesis since it is found in bound form to pre-ribosomal RNA [149-153]. Later it has been shown that overexpression of nucleolin is linked with upregulation of RNA polymerase I, which takes part in transcription of ribosomal RNA [154, 155]. In addition to that, downregulation of nucleolin causes growth arrest or increased apoptosis rate [156, 157]. Later studies revealed that, especially on cancer cells, upregulated expression of nucleolin has been reported on the cell membrane in addition to nucleolus [146, 152, 158, 159].

As stated above, cancer cell specific anti-proliferative effect of GRO's has been shown. Later, effect of GRO's on S-phase arrest on cancer cells has been reported [160]. When AS1411 interacts with nucleolin on cell surface, it is internalized and its interaction with nuclear factor-κB (NF- κB) essential modulator, which is a regulatory subunit of the inhibitor of κB kinase complex, has been shown [147, 161]. Girvan et al. reported that, by inhibition of IKK complex, apoptosis is induced [147]. In addition to that, while in cancer cells *bcl-2* mRNAs are stabilized by overexpressed nucleolin protein, on AS1411 exposed cancer cells, decreased half-life of *bcl-2* mRNA has been shown. Similar results also obtained by nucleolin knockdown on same cell lines [162-164].

Aptamer AS1411 is uptaken into the cell via macropinocytosis pathway on cancer cells in which cell engulfs surrounding medium with its content with a signal dependent process mediated by AS1411 internalization by nucleolin in this case, while it is uptaken into healthy cells by non-macropinocytosis. Internalization of AS1411 by macropinocytosis causes more macropinocytosis due to increased activation of Rac1. Reyes-Reyes et al has shown that, specific anti-proliferative effect of aptamer on cancer cells is in relation with the internalization method [165, 166]. Same research group later showed that, nucleolin inhibition by siRNA or aptamer AS1411 increases activation of Rac1, which is a protein from Ras superfamily taking part in cell growth and cytoskeletal reorganization, also upregulated in breast cancer [167], and increased Rac1 activation upregulates macropinocytosis pathway and leads methuosis, a non-apoptotic cell death occurring due to excess macropinocytosis [167-170].

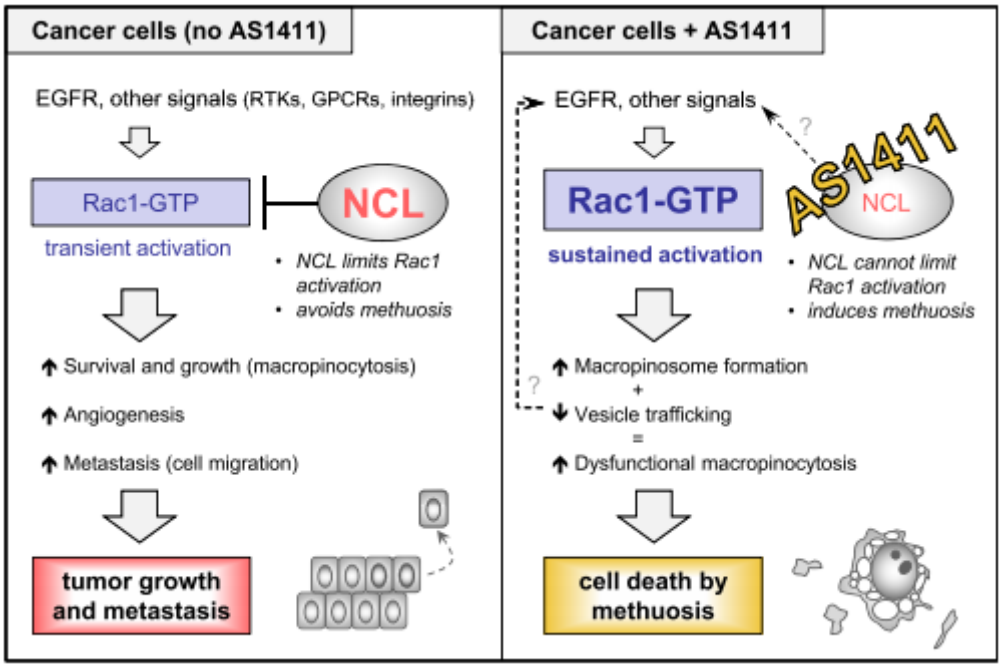

Figure 1.2. AS1411 mechanism of action [170]

In addition to cancer cell specific anti-proliferative effect, aptamer AS1411 also used as a targeting agent in conjugation to nanostructures like drugs, gold nanoparticles, micelles, and mesoporous silica [141]. In this study, aptamer AS1411 will be used as both a targeting agent in conjugation to mesoporous silica which carries anti-cancer drug and a nanovalve system controlling actively drug concentration by cancer cells.

1.5.2. Controlled Release

Current cancer therapeutics like doxorubicin and paclitaxel have severe side effects due to accumulation of drug on healthy tissue and lack of targeting as stated above. With the usage of nanotechnology in medicine in recent years, drug carrying nanoparticles, ranging from 1-100nm in size [171-173], have been developed and used to decrease those side effects and provide more efficient therapy. Nanoparticles have been studied extensively by encapsulation of drugs and facilitating release of drugs around the targeted tissue which also provides better imaging tools for cancer diagnosis [174-179]. For those purposes nanoparticles with different chemical properties such as carbon nanotubes [180], liposome

based carriers [181, 182], hydrogels [183], polymeric nanoparticles [184], dendrimers [185], micelles [186] and mesoporous silica nanoparticles [187-189] have been studied.

Studies showed that, using those nanoparticles as drug carriers contributes higher efficacy and decreases side effects. Moreover, nanoparticle usage increases solubility of poorly soluble drugs [190, 191], increases half-life of drug [46, 192] increases uptake of drugs into target cells [193] and overcomes drug resistance [194]. In addition to benefits of nanoparticle usage, to keep drug concentration in therapeutic range, several strategies for controlled release have been used [195, 196]. Controlled release profile can be obtained by several methods like pH dependent release [197], temperature dependent release [198], light dependent release[198]. To illustrate those concepts, few studies using those strategies are explained below. In this thesis study, for the first time, the efficiency of stimuli dependent switchable aptamer nanovalve system was determined on cancer cells and targeting capability of this switchable system was tested in vivo.

Carbon nanotubes are formed by sheets of benzene rings resulting in single or multi-walled carbon nanotubes. Due to unique physicochemical properties of carbon nanotubes, they have been used for diagnosis, drug delivery and imaging studies [192]. Those properties include ultralight weight, high surface area, thermal and electrical conductivity due to carbon-based structure [180, 194, 199]. Liu et al showed that, paclitaxel release from carbon nanotubes was significantly higher in mouse serum, and significant reduction on tumor growth on mice treated with paclitaxel-carbon nanotubes [192, 200]. However, studies showed that, carbon nanotubes also induced DNA damage and cell death in normal human dermal fibroblast cells [201, 202]. Moreover, carbon nanotubes show poor solubility with common solvents such water and organic solvents [203].

Liposomes are formed by one or more lipid bilayers with aquatic phase in between each layer [46]. Due to presence of both hydrophilic and hydrophobic layers, liposome-based nanoparticles can transfer wide range of substances in respective layer. Moreover, liposomes are self-assembled, biocompatible, and biodegradable [182, 204]. Liposomes are extensively studied, and several liposome-based drugs have been approved by FDA [182]. Layek et al reported that, tamoxifen citrate release on sustained release profile has been observed form liposome based delivery system [205].With the surface modifications, liposome derivatives are developed to release their cargo on certain pH or temperature. Even though liposome surface can be also modified via targeting agents, active targeting could not be achieved in

clinics via liposome-based nanoparticles due to clearance of drug and limited accumulation on tumor site [182].

In the present study, Mobile crystalline material (MCM-41 type) mesoporous silica nanoparticles are used to encapsulate anti-cancer agent. MCM-41 type silica nanoparticles are Silicon dioxide based and they have hexagonal structure. They have several advantages over other nanoparticles such as high surface area/volume ratio, structured pore size, stability, and biocompatibility in addition to silanol containing surface which facilitates functionalization of nanoparticle via surface modifications [206, 207]. Numerous studies showed that, therapeutic drug loaded MCM-41 type silica nanoparticles increase uptake and provide better drug encapsulation and release profiles [208-214].

Mamaeva et al recruited γ-secretase inhibitor loaded mesoporous silica nanoparticles to target notch signaling which is upregulated on breast cancer [177]. Even though γ-secretase inhibitors show severe side effects when used as a free drug due to active notch signaling on many tissues, researchers successfully targeted breast tumor with the nanoparticle. In comparison to free drug, enhanced therapeutic effect has been reported.

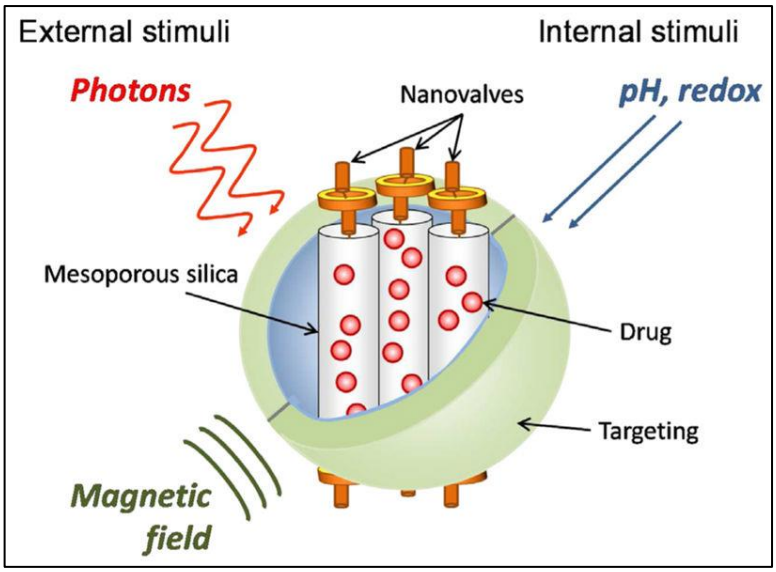

Figure 1.3. Controlled release strategies for silica nanoparticles [188]

In addition to properties of MCM-41 type silica nanoparticles by themselves, controlled release profile can be obtained by molecular gates which prevents drug release before extrinsic signal acquired by the carrier molecule. Control release of drug aims to minimize

premature release of drug in the body before nanoparticles reach the targeted tissue. In this way, highest efficacy with minimum drug concentration can be achieved [215]. For MCM-41 type silica nanoparticles, multiple strategies are being followed to reach targeted drug release. Mainly, surface modifications work as nanovalves by closing pores on silica nanoparticles and preventing drug release in absence of stimuli. When targeting molecules on the surface of silica nanoparticles interact with target molecule, pores open and drug release occurs depending on the stimuli. Primary methods developed for targeted and controlled release are irreversible due to chemical reactions or weakened interactions of targeting molecules [216]. Newer methods provide controlled release via reversible nanovalves, thus providing higher control over release profile [216-219]. Also, there are some studies conjugating drug to silica surface instead of encapsulating, then provide release by disrupting conjugation between drug and silica nanoparticle via stimuli [220].

pH dependent controlled drug release has been studied due to acidic pH of tumor microenvironment and intracellular lysosomal compartments [220]. While Zhang et al recruited doxorubicin conjugated silica nanoparticles, Zhao et al used pH (low) insertion peptide silica nanoparticle conjugates for pH dependent controlled release. Both studies showed that, as nanoparticles enter acidic tumor microenvironment, pH change disrupts bonds on silica nanoparticle and controlled doxorubicin release profile can be obtained. By those methods decrease on viability of breast cancer cells reported with controlled drug release [220, 221]. However, both strategies use nanoparticles which release doxorubicin in an irreversible manner. This release profile may not be efficient for doxorubicin resistant breast cancer cells as shown by Zhao et al, efficacy is less for doxorubicin resistant MCF-7/ADR cells in comparison to doxorubicin sensitive MCF-7 cell line [221].

Moreover, silica nanoparticles can be functionalized with magnetic field sensitive capping [222], thermoresponsive capping [223], UV light sensitive capping [224] strategies have been researched. However, similar to pH sensitive drug release systems, majority of surface modifications do not provide reversible controlled release properties.

Aptamers have been also used as molecular gates by several studies due to their ability to target specific molecules and their nucleotide based flexible structure [225, 226]. In this study, previously developed AS1411 aptamer- MCM-41 type silica nanoparticle conjugate will be further studied. In the study of Hernandez et al, engineered AS1411 aptamer was used as a molecular gate on drug loaded mesoporous silica nanoparticle [227]. Additional 7

nucleotides on 5’ end of AS1411 aptamer provided capability to act as a nanovalve on pores of MCM-41 type silica nanoparticles. Obtained hairpin structure prevented drug release from mesoporous silica nanoparticles in natural conformation of aptamer. When modified AS1411 aptamer interacts with its target, nucleolin protein, due to conformational change on modified aptamer, cargo of silica nanoparticles was released as it has been shown with fluorescein in their study. Hernandez et al successfully showed the ability of delivery complex to target nucleolin positive MDA-MB-231 cells in comparison to nucleolin negative MCF-10A cells.

Therefore, in the present study, firstly we examined targeting ability and cellular uptake of AS1411 Aptamer-MCM-41 type silica nanoparticle (Apta-NP) complex on nucleolin positive triple negative murine breast cancer cells, E0771, by fluorescence microscopy and flow cytometry. Then we showed cytotoxic effect of Apta-NP complex on E0771 cells in comparison to free drug via WST-1 cell viability assay. Thereupon we evaluated the in vivo controlled drug delivery and release potential of Apta-NP complex via in vivo fluorescence imaging on E0771 allograft breast cancer model we constructed on mice.

2. MATERIALS AND METHODS

2.1. MATERIALS

2.1.1. Consumables

Table 2.1. Consumables used for cell culture experiments

#	Brand	Item	Catalog No
1	TPP	Cell culture Flask T75, T25	90075-25
2	SPL	Serological Pipette 5ml, 10ml, 25ml	91005,10,25
3	CAPP	Microcentrifuge tubes 1.5ml, 2ml	5101550C, 52000C
4	Axygen	Micropipette tips 10ul, 200ul,1000ul	301-03-051
5	Axygen	Falcon 15ml, 50ml	SCT15ML25S
6	SSI BIO	Falcon 5ml	1410-09
7	Isolab	Cryotube (2ml)	I.091.11.102.100
8	FinnPipette	Micropipette (2ul, 20ul, 200ul, 1000ul)	4642010,50,80,90
9	Corning	6 Well plate,	3516
10	Costar	96 Well plate	3596
11	Sigma	Haemocytometer	Z359629
12	Isolab	Pipette Pump	010.01.006

2.1.2. Chemicals

Table 2.2. Chemicals used for cell culture experiments

#	Brand	Item	Catalogue No
1	Gibco	RPMI1640	21875034
2	Gibco	FBS	10500064
3	Gibco	PBS	13190094
4	Gibco	Pen/Strep	15140122
5	Gibco	Trypsin	25200056
6	Sigma	DMSO	D8418
7	Vectashield	DAPI	H-1200
8	Roche	WST-1	11644807001
9	Honeywell Fluka	Fluorescein	28803
10	Sigma	Paclitaxel	T7402

2.1.3. Instruments

Table 2.3. Instruments used in experiments

#	Brand	Item	Catalogue No
1	Esco	Cell Culture Hood	Class II BSC
2	Sigma	Centrifuge	3-18K
3	Haier -86 UltraFreezer	UltraFreezer	DW86L338
4	Panasonic	-20 Freezer	MDF-U731M
5	Arçelik	Fridge	No-Frost
6	Esco	Cell culture Incubator	CCL-050B-8
7	American Optical Corporation	Light Microscope	1810
8	Zeiss	Fluorescent Microscope	Discovery.V20
9	ThermoFisher Scientific	Spectrophotometer	VL0L00D0
10	Beckman Coulter	Flow cytometry	CytoFLEX S
11	IVIS	In vivo imaging	Illumina Series III
12	Leytemed	Water bath	DK-420-CE
13	Nalgene	Cell freezing	5100-0001

2.1.4. Cell Line

- E0771 Murine Triple Negative Breast Cancer (CH3-Biosystems, 940001)

2.2. STUDY DESIGN

In this study, effects of aptamer mediated drug carrying silica nanoparticles (Apta-NP complex) on targeting, uptake, localization, and cytotoxicity were examined in nucleolin positive murine breast cancer E0771 cells. To investigate effect of Apta-NP complex on cellular uptake, flow cytometry was utilized on cells treated with either Apta-NP-Fl complex or NP-Fl. Then, cells were exposed to same delivery complexes to visualize localization of fluorescein cargo released from Apta-NP-Fl and NP-Fl using fluorescence microscopy. To examine the cytotoxicity of aptamer-gated drug delivery complex on murine triple negative breast cancer cells, E0771 cells were incubated with either Apta-NP-TXL delivery system or free TXL with equal amount of paclitaxel concentration in the range of 0 to 100 µM. In addition, to investigate in vivo targeting ability of aptamer-gated drug delivery complex,

E0771 cells were inoculated into right flank of female C57BL/6 mice and tumor growth was examined. When tumors reach palpable size (≈150mm^3), Apta-NP-Fl was injected subcutaneously, and localization of fluorescein was performed using in vivo imaging techniques with one-hour intervals up to four hours. Also, one final image of the fluorescent signal was acquired after 24 hours of Apta-NP-Fl injection.

2.3. CELL MAINTENANCE

E0771, Triple negative murine breast cancer cell line was kindly provided by Prof. Dr. Margot P. Cleary at Hormell Institute Medical Research Center, University of Minnesota, Austin, United States. Frozen cells were thawed at gentle agitation in 37°C water bath. Then content of cryotube was transferred into 15 ml centrifuge tube with nine ml of RPMI 1640 medium with 10 per cent FBS and one per cent Pen/Strep. Then, cell suspension was centrifuged at 300 g (1200 rpm) for five minutes. Afterwards, supernatant was removed, and pellet was dissolved in fresh medium and resuspended in appropriate flasks. Throughout the study cells were incubated in T75 flasks at 37°C in five per cent CO_2 incubator. Cell culture medium replenished every two or three days and cells were sub-cultured when they reached up to 80 per cent confluency. For sub-culturing, medium was removed then cells were washed with PBS and treated with one ml of trypsin to detach them. Later, T75 flask was shaken gently to spread trypsin on the cell surface. After three to four minutes of incubation in cell culture incubator at 37°C, cells were resuspended in fresh medium. Hemocytometer was utilized for cell count. After calculation of cell concentration in the resuspension, cells were transferred to appropriate centrifuge tubes and centrifuged for further processes. To freeze and store cells, freezing medium was prepared by mixing 10 per cent DMSO and 90 per cent complete RPMI 1640 medium. 1.5 million cells were resuspended in one ml of freezing medium and mixture is transferred into cryotubes. Cryotubes were stored in cell freezing chamber overnight before they are transferred to ultra-freezer. For the experiments in this master's thesis study, cell passage numbers from 5 to 15 were used.

2.4. CHARACTERIZATION OF APTA-NP DRUG DELIVERY SYSTEM

Characterization of MCM-41 type silica nanoparticles and Apta-NP drug delivery system were performed by using Transmission Electron Microscopy (TEM), Scanning Electron Microscopy (SEM), Atomic Force Microscopy (AFM), Dynamic Light Scattering (DLS) and Fourier-Transform Infrared Spectroscopy (FTIR). Then drug release from Apta-NP-TXL. Cellular fluorescein uptake in presence of Apta-NP-Fl or NP-Fl drug delivery systems were measured by both flow cytometry and fluorescence microscopy. And TXL release from Apta-NP-TXL drug delivery system in comparison to NP-TXL system was measured via spectrophotometry.

2.4.1. TEM Analysis

TEM analysis were performed to characterize compositional and crystalline properties of MCM-41 type silica nanoparticles used in present study. Particles were prepared by ultrasonication of silica nanoparticle powder in ethanol for 5 minutes. Then, droplet of suspension was dried on a standard holey carbon TEM grid. Analysis were carried out on Titan 60-300 electron microscope (FEI, Netherlands) operating at 300kV in TEM mode.

2.4.2. SEM Analysis

SEM analysis of MCM-41 were performed to characterize surface properties. Analysis were done with Zeiss EVO LS 10 microscope under high vacuum conditions with 30,000 X magnification.

2.4.3. AFM Analysis

To further analyze surface properties of MCM-41 type mesoporous silica nanoparticles, AFM was used for nanometric imaging in dry form by using ezAFM (Nanomagnetics Instruments, Ankara, Turkey).

2.4.4. DLS Analysis

Average size distribution of MCM-41 type silica nanoparticles, DLS analysis were performed with Zetasizer Nano-S (Malvern Instruments, Worcestershire, UK).

2.4.5. FTIR Analysis

Amino-functionalization of MCM-41 type mesoporous silica nanoparticles was analyzed via FTIR.

2.4.6. Measurement of Cellular Uptake of Apta-NP-Fl by Flow Cytometry

Nucleolin positive E0771 cells ($150x10^3$cells/well) were cultured in six well plates and incubated overnight at 37°C. The next day, cells were treated with 0, 10, 25 or 50 µg/ml fluorescein loaded Apta-NP or fluorescein loaded only NP for two hours. Then, cells were collected with complete RPMI medium after trypsinization and centrifuged at 1500 rpm for five minutes. Following that, supernatant was removed, and cells pellet was re-suspended in 500 µl 4 per cent PFA and incubated for 15 minutes. Then cells were centrifuged again at 1500 rpm for five minutes. Supernatant was removed, and pellet was resuspended in 200µl PBS. Resuspended cells were transferred to 96 well plate for flow cytometry analysis. Beckman Coulter flow cytometry was used for experiments. At least $5x10^5$ events per well was read. Sample with no fluorescein treatment was used as unstained negative control. Experiments were repeated three times and data points were calculated as mean ± standard error. Results were collected as dot plots.

2.4.7. Determination of In Vitro Localization and Targeting Ability of Apta-NP System by Fluorescence Microscopy

Total of 150 x 10^3 of E0771 cells in RPMI 1640 medium with 10 per cent FBS and one per cent Pen/Strep were cultured on six well plates. The next day, cells were incubated with 0, 10, 25 or 50 µg/ml either fluorescein loaded Apta-NP-Fl or NP-Fl for two hours. Then, medium was removed, and cells were washed with PBS twice. For fixation, cells were

treated with 4 per cent PFA for 15 minutes. Following that, cells were washed with PBS again and few drops of DAPI was added to each well. Visualization of Apta-NP-Fl uptake was examined by fluorescence microscope. DAPI and FAM channels were used separately, and images were merged later on FIJI-Image-J.

2.5. MEASUREMENT OF CYTOTOXICITY OF APTA-NP-TXL ON BREAST CANCER CELLS

Apta-NP drug delivery system consists of, MCM-41 type mesoporous silica nanoparticle, AS1411 aptamer and loaded drug. This study aims to show that, paclitaxel loaded aptamer-gated nanovalve system has higher toxicity in comparison to free paclitaxel at same dose. To eliminate effect of silica nanoparticle on cytotoxicity of Apta-NP drug delivery system, total of 5×10^3 E0771 cells were seeded on each well of 96 well plate and exposed to MCM-41 type silica nanoparticles up to 100 µM after adhesion of cells. All doses were performed as triplicates. Cells are incubated at 37°C for 24 or 48 hours with drugs. Following that 10 µl of WST-1 reagent was added to each well at the end of incubation period via multichannel pipette in dark. 96 well plate was gently shaken to mix WST-1 reagent with the medium and incubated at 37°C for one more hour. Then, 96 well plate was covered with aluminum foil to prevent light exposure and absorbance was measured at 440nm using spectrophotometry. For each concentration, average absorbance values of the samples were normalized to average absorbance values of control group (0.1 per cent DMSO, complete medium). Then percent survival in comparison to control group for each treatment was calculated. Experiments were repeated three times and data points were calculated as mean ± standard error.

Following that, effect of paclitaxel loaded Apta-NP drug delivery system (Apta-NP-TXL) on cytotoxicity was examined in comparison to free drug. Paclitaxel (TXL) powder was dissolved in DMSO as a stock solution and diluted in complete RPMI medium in the range of 0-100µM concentration for in vitro cytotoxicity study. The same Paclitaxel (TXL) stock solution was also used to prepare Apta-NP-TXL solution. To measure cell viability, total of 5×10^3 E0771 cells were seeded in each well of 96 well plate and then cells were incubated at 37°C in complete medium overnight. WST-1 procedure applied for cytotoxicity of silica nanoparticles stated above was also followed for this experiment. In order to detect dose

dependent cytotoxicity of Apta-NP-TXL, eight different concentrations of TXL at 0, 1, 2.5, 5, 10, 25, 50, 100 uM was used. Experiments were performed as triplicates for each concentration. After either 24 or 48 hours of incubation in 37°C incubator.

2.6. IN VIVO EXPERIMENTS

2.6.1. Animals

All animal experiments in this study has been approved by Yeditepe University Ethical committee (Decision no: 22.7.2016/554). For the study, eight to ten-week-old female C57BL/6 mice were cared under the supervision of Yeditepe University Medical School, Experimental Research Center (YÜDETAM). All animals were fed with ad libitum food and water.

2.6.2. Allograft Tumor Model

After primary body weight measurement, healthy eight to ten-week-old female mice were subcutaneously inoculated on right flank region with 100 µl, with $1x10^6$ freshly trypsinized E0771 cells by using one ml sterile insulin injector. After cell inoculation, animals were examined every three days for body weight changes and tumor growth.

2.6.3. In Vivo Imaging

When tumor growth reaches palpable size (around $150mm^3$, measured by a x b x c /2). Due to dark hair color of mice, front region was shaved with a razor. Then, Apta-NP-Fl complex was subcutaneously injected to mice. After Apta-NP-Fl injection (t=0h), an in vivo fluorescent image from both dorsa-ventral and ventra-dorsal directions has been acquired for four hours following injection with one-hour intervals at 480-580nm by IVIS Ilumina Series III at Boğaziçi University Center for Life Sciences and Technologies (Vivarium). At the end of 24 hours, one last image was acquired then animals were sacrificed and organs like brain, hearth, liver, and tumor were collected for histopathologic analysis.

2.7. STATISTICAL ANALYSIS

Prism Software version 7.00. was utilized to perform statistical analysis of the present study. Results of the experiments of this study were shown as mean ± SD. For cytotoxicity assay, two-way ANOVA test was done. For multiple comparisons, Tukey's Test was performed as post-hoc test. For IC50 calculation, log (TXL concentration) vs response (per cent survival) was used in Prism. "n" value represents the number of the repeated experiments as it has been stated in figure legends and figure captions. In addition to that, samples were used as triplicated during each experiment. Means of the triplicated were used during statistical analysis. P value is equal or smaller than 0.05 ($p \leq 0.05$) was accepted as statistically significant.

3. RESULTS

Specific targeting ability of MCM-41 type mesoporous silica nanoparticles functionalized with nucleolin targeting aptamer, AS1411, as nanovalves (Apta-NP) has been shown on nucleolin positive breast cancer cells [227]. In this study, cytotoxic effect of drug loaded Apta-NP drug delivery system was shown on E0771, triple negative, nucleolin positive murine breast cancer cell line. Then, in vivo targeting ability of the Apta-NP system was shown on allograft mouse breast cancer model.

3.1. CHARACTERIZATION OF APTA-NP DRUG DELIVERY SYSTEM

In this study, Apta-NP drug delivery complex was synthesized as previously described [227]. Characterization of MCM-41 type mesoporous silica nanoparticles were done by using several methods. Firstly, TEM images showed that, silica nanoparticles show typical hexagonal nanopores (Figure 3.1) [228].

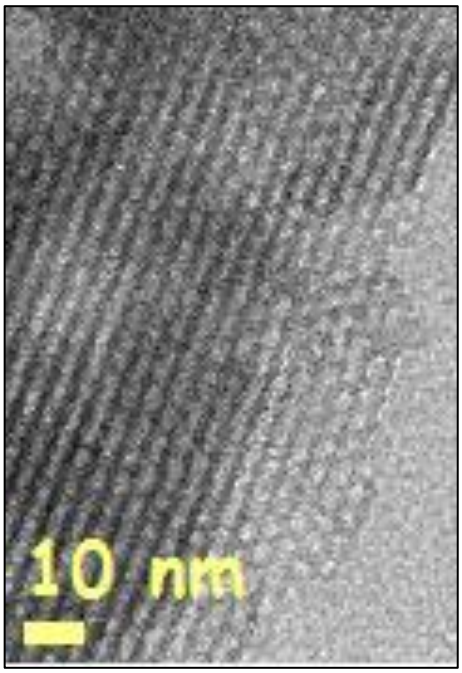

Figure 3.1. TEM images MCM-41 type mesoporous silica nanoparticles used in current study [228, 229]

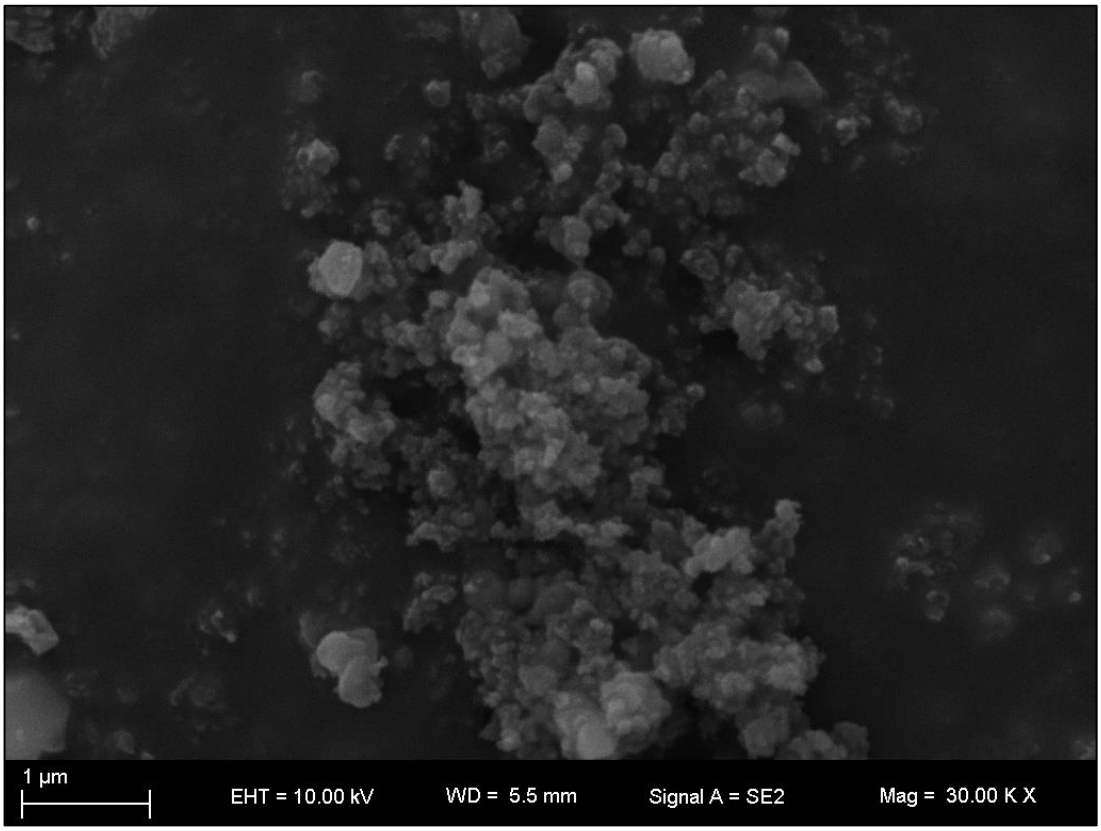

Figure 3.2. SEM images of MCM-41 type mesoporous silica nanoparticles used in current study [228, 229].

SEM was used to examine surface properties and size of the MCM-41 type silica nanoparticles, round, spherical particles have been observed (Figure 3.2) [228]. Following SEM analysis, AFM was utilized to examine particles. Maximum height of particles was ranging from 20-200 nm (Figure 3.3) [228]. Average hydrodynamic diameter of MCM-41 type nanoparticles was measured via DLS was 191 ± 1.3 nm (Figure 3.4) [228]. Following those, amino functionalization of silica nanoparticles was shown via FTIR spectra (Figure 3.5) [228]. Bands on 1460 and 690 nm seen on FTIR spectra shows N-H asymmetric bending vibrations and N-H bending which are typical to amino group addition on silica nanoparticle surface [230].

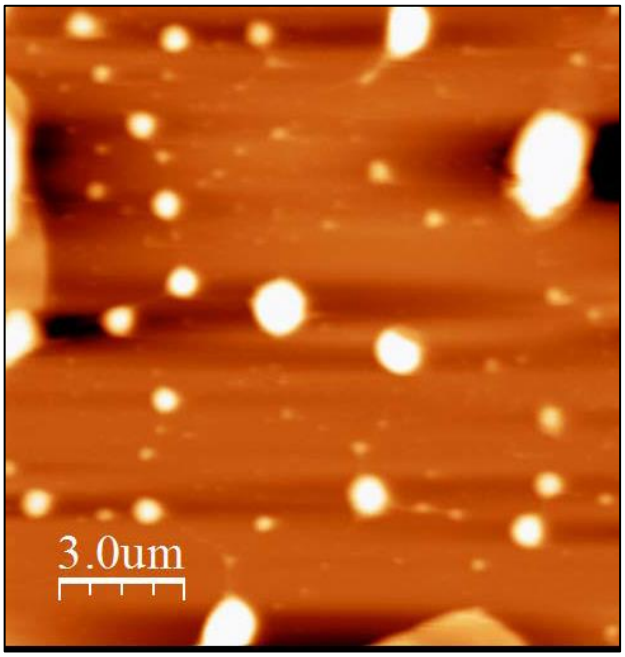

Figure 3.3. Nanometric imaging of MCM-41 type mesoporous silica nanoparticles used in current study by AFM [228, 229].

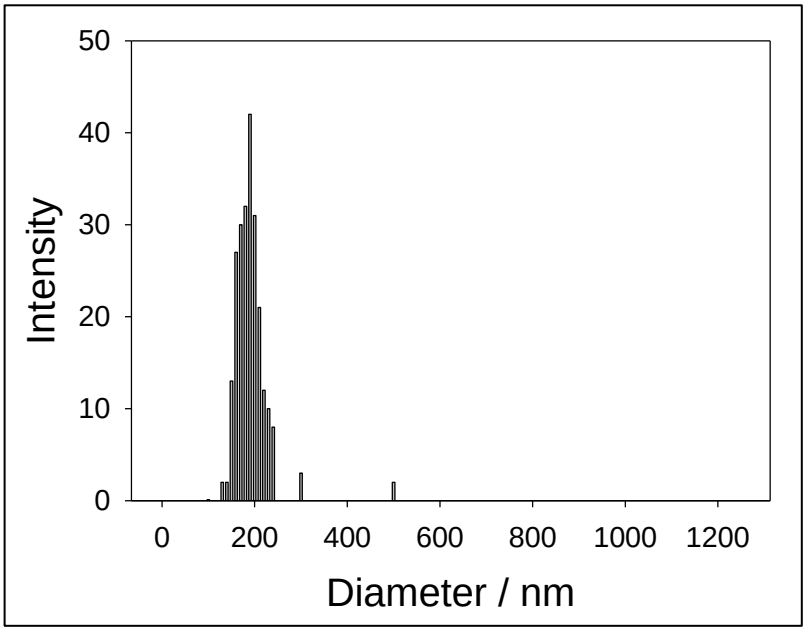

Figure 3.4. Average diameter of MCM-41 type mesoporous silica nanoparticles used in current study by DLS [228, 229].

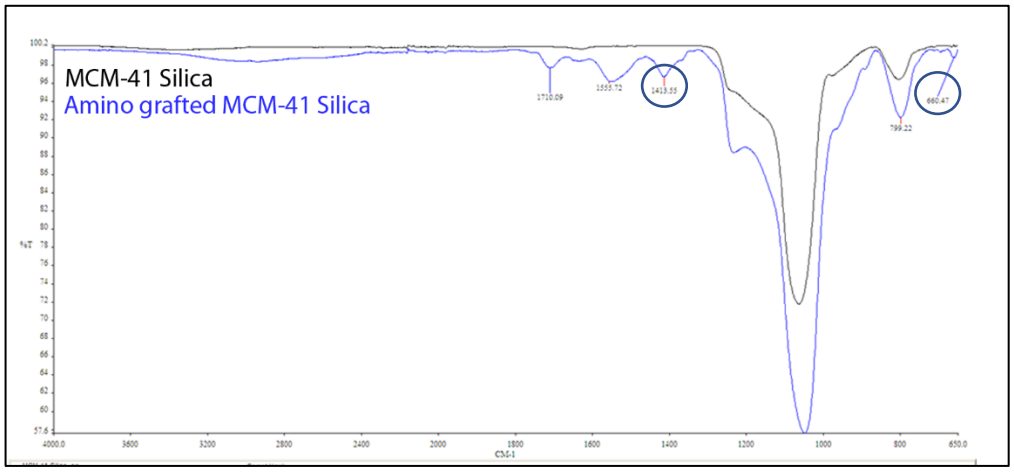

Figure 3.5. FTIR spectra of MCM-41 type mesoporous silica nanoparticles after amino grafting [228, 229].

3.1.1. In Vitro Uptake

To demonstrate targeting ability of aptamer gated drug delivery system, firstly we utilized flow cytometry after treating E0071 cells with 0-50 µg/ml Apta-NP-Fl or NP-Fl for two hours. Then, fluorescein stained cell percentage was measured quantitatively by flow cytometry. Representative results are shown in Figure 3.7. As the fluorescein concentration increased, increased uptake on both Apta-NP-Fl and NP-Fl groups were measured. Higher uptake on cells incubated with Apt-NP-Fl was shown in comparison to cells incubated with same concentration of fluorescein carrying NP-Fl ($p>0.05$) (Figure 3.8).

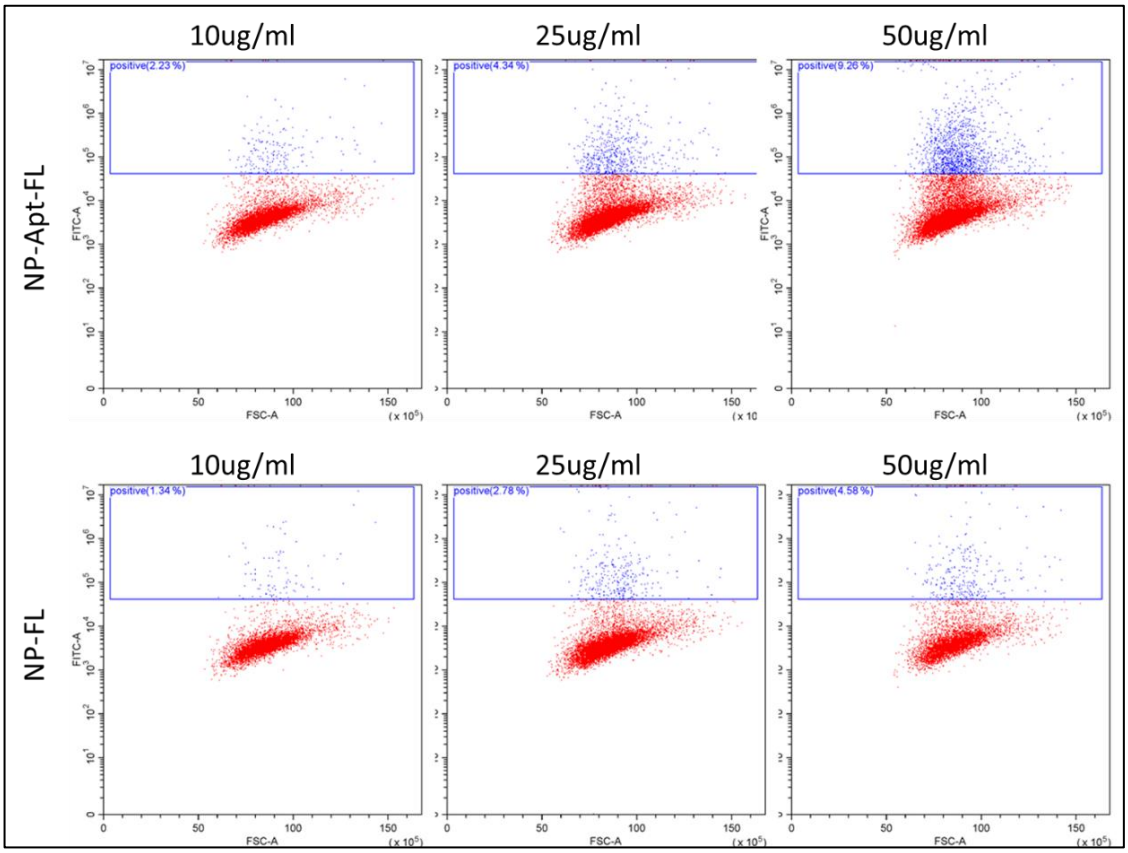

Figure 3.6. Representative dot plots of fluorescein uptake of E0771 cells incubated with NP-Fl or Apta-NP-Fl delivery system. Top panel refers to incubation of cells with NP-Apt-Fl while bottom panel refers to NP-Fl incubation with equal concentration of fluorescein (10, 20 or 50 µg/ml). Untreated cells were used as unstained negative control.

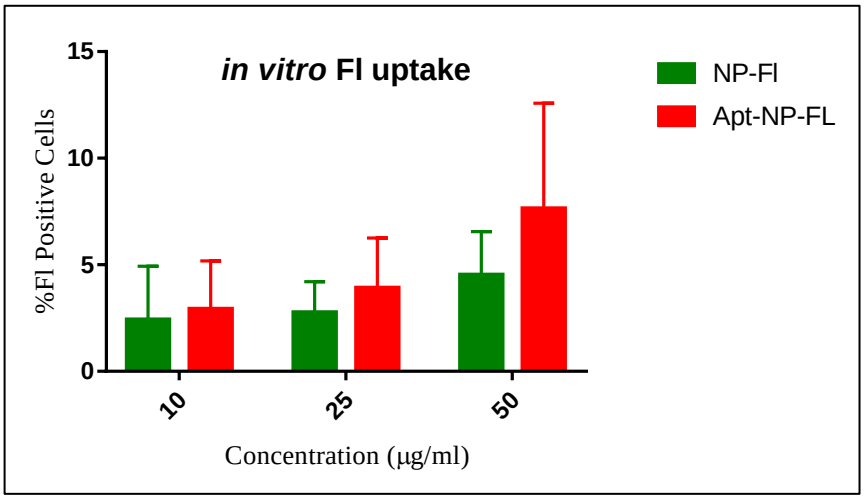

Figure 3.7. Quantification of in vitro fluorescence uptake of E0771 cells. (Green: NP-Fl treatment, Red: Apta-NP-Fl treatment). For statistical analysis, t-test was performed. ($p>0.05$, $n=3$).

3.1.2. In Vitro Localization

To examine cellular localization and uptake of fluorescein by aptamer gated drug delivery system in comparison to NP-Fl, fluorescence microscopy was used. Similar to in vitro uptake experiment, E0771 cells were incubated with 10, 25 or 50 µg/ml fluorescein carrying Apta-NP-Fl or NP-Fl drug delivery complexes for two hours. Representative fluorescence microscopy images are shown in Figure 3.9. DAPI channel and FAM channel were used separately during experiments, merged DAPI/FAM images are shown below. Intense fluorescence signal was detected on cells treated with Apta-NP-Fl even in 10 µg/ml and increasing fluorescence intensity was observed in higher doses for this treatment. In comparison to Apt-NP-Fl treatment, lower fluorescence intensity was observed on cells treated with NP-Fl. With this experiment, increased uptake of fluorescein by Apta-NP-Fl treated cells and localization of fluorescein around the nucleus has been shown.

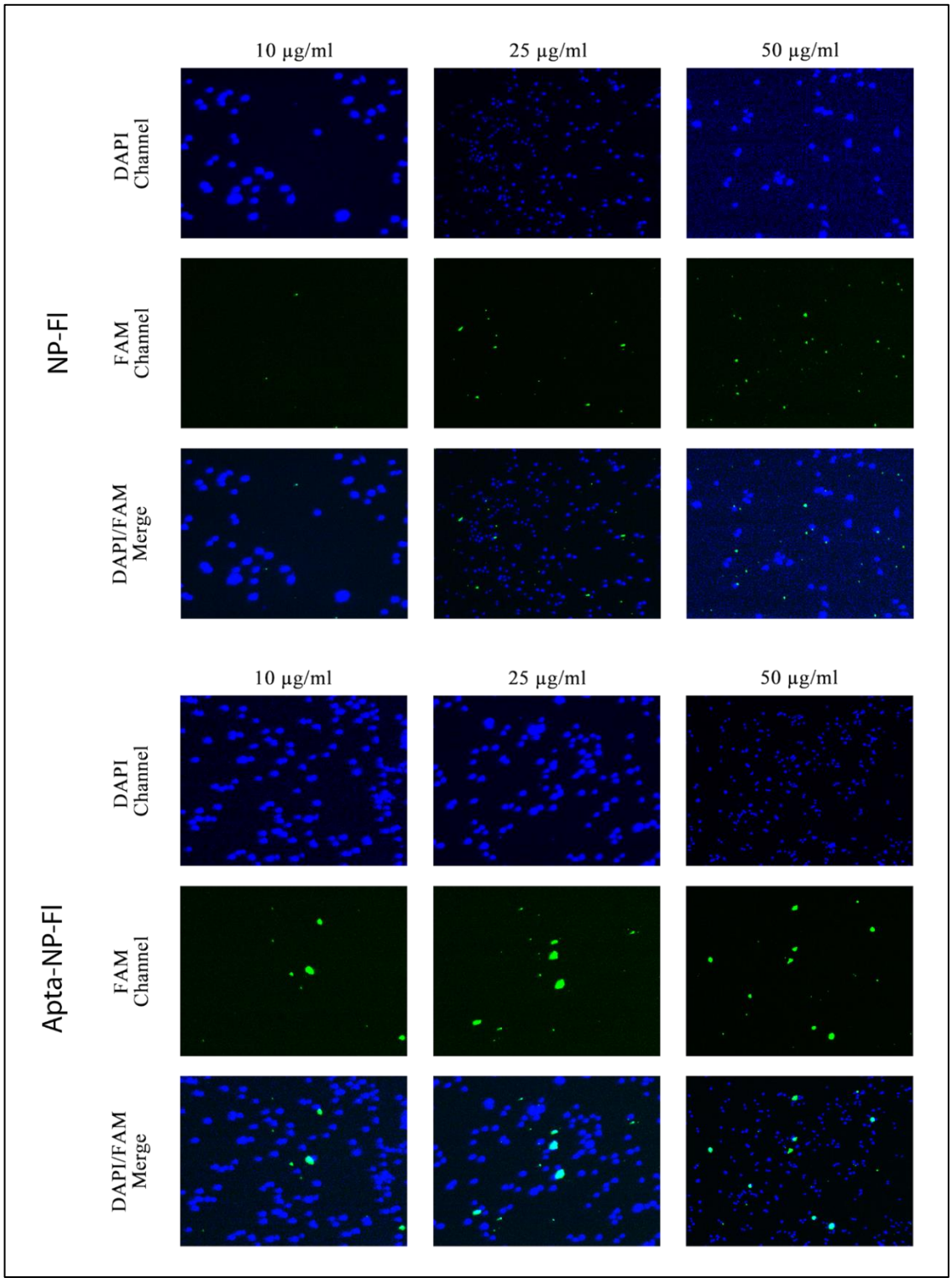

Figure 3.8. In vitro uptake and localization of Fluorescein (10, 25 and 50 µg/ml). Images obtained from NP-Fl treatment are shown on top panel as images from Apt-NP-Fl treatment are shown on the bottom panel.

3.1.3. Measurement of Drug Release from Apta-NP-TXL Drug Delivery System

For time dependent drug release experiment, Apta-NP-TXL and NP-TXL drug delivery systems were used. It has been shown that, drug release from NP-TXL occurs immediately in high percentage, which decreases the efficiency of drug delivery, while, effective capping of Apta-NP-TXL drug delivery system inhibits drug release from the system. When Apta-NP-TXL complex is exposed to target protein, nucleolin, drug release occurs as shown in Figure 3.6.

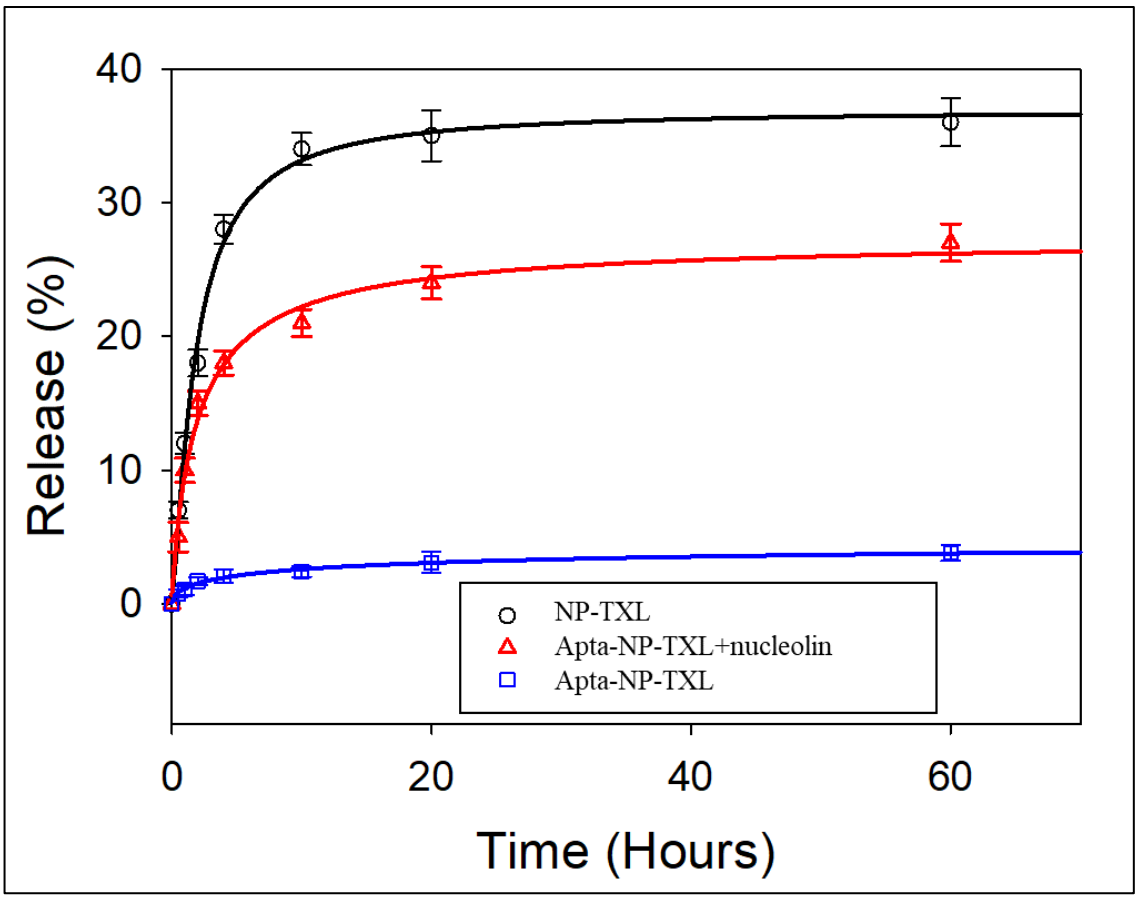

Figure 3.9. Time dependent drug release from Apta-NP-TXL complex in the presence of target in comparison to NP-TXL.

3.1.4. Cytotoxicity of MCM-41 Type Silica Nanoparticles

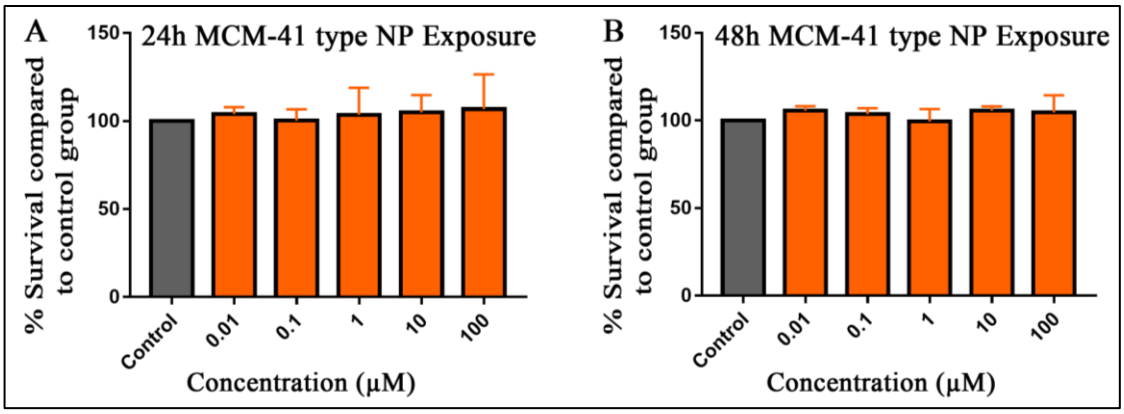

Figure 3.10. Effect of MCM-41 type NP exposure on cell viability in comparison to 0.1% DMSO treated control group. E0771 cells were treated with increasing concentration of MCM-41 type silica nanoparticles up to 100 µM. a) Cell survival after 24 hours of MCM-41 type silica nanoparticle exposure. B) Cell survival after 48 hours of MCM-41 type silica nanoparticle exposure. * indicates significant difference in comparison to control group. *$p<0.05$, by one-way ANOVA compared to control group, n=3.

To evaluate possible cytotoxic effect of MCM-41 type silica nanoparticles on E0771 cells, WST-1 assay was performed to compare cell viability in comparison to non-treated group. Cells were exposed up to 100 µM MCM-41 type silica nanoparticles for 24 or 48 hours. Assays were performed as triplicates and obtained data was normalized to cells incubated without MCM-41 type silica nanoparticles. In Figure 3.4 we demonstrated that, there is no significant difference between viability of cells incubated with silica nanoparticles and 0.1% DMSO treated control group. Those results show that, mesoporous silica particles do not show any cytotoxicity on E0771 cells. Thus, increased cytotoxicity of aptamer-gated nanovalve complex on E0771 cells as shown below is not due to the presence of silica nanoparticles and caused by aptamer-gated nanovalve.

3.1.5. Cytotoxicity of Paclitaxel Loaded Aptamer-Nanoparticle Complex

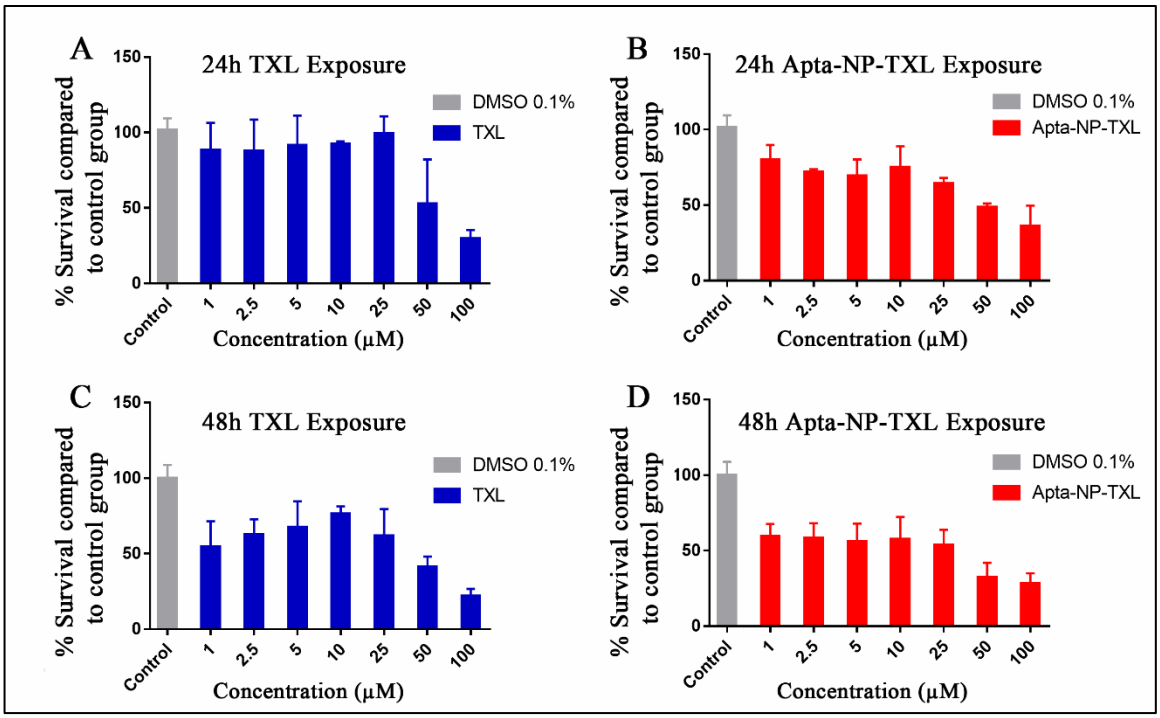

Figure 3.11. Effect of Apta-NP -TXL exposure on cell viability. E0771 cells were treated with increasing concentration of Apta-NP -TXL complex or free TXL up to 100 µM. A) Cell survival after 24 hours of free TXL. B) Cell survival after 24 hours of Apta-NP-TXL. Two-way ANOVA with Dunnett multiple comparison was performed for statistical analysis. C) Cell survival after 48 hours of free TXL. D) Cell survival after 48 hours of Apta- NP-TXL. * indicates significant difference in comparison to control group (*$p<0.05$, n=3).

Wst-1 assay was performed to measure cytotoxicity of Apta-NP-TXL complex on E0771 cells in comparison to free TXL treatment. Cells are incubated with 0-100 µM TXL loaded Apta-NP-TXL or free TXL for 24 or 48 hours. Assays were performed as triplicates and obtained data was normalized to cells incubated without drugs. Higher cytotoxicity of Apta-NP-TXL complex against E0771 cells was shown in Figure 3.11. While percent survival in comparison to control group is significantly different for all doses from 2.5 µM (except 10 µM) for Apta-NP-TXL treatment, only 50 µM and 100 µM free TXL treatment showed significant toxicity in comparison to control group for 24 hours of treatment.

Table 3.1. Comparison of IC50 values for Apta-NP-TXL or free TXL treatment

IC 50	Free TXL (µM)	Apta-NP-TXL (µM)
24h	45.76	36.41
48h	48.87	35.64

For 48 treatment, both treatments showed significant toxicity in comparison to control group for every dose. However, as shown in Table 3.1, IC50 value for free TXL was 45.76 µM and 36.41 µM for Apta-NP-TXL. After total 48 hours of incubation with drugs, IC 50 value for free TXL was 48.87 µM while it was 35.64 µM for Apta-NP-TXL. For both experiments aptamer-based nanovalve system shows superiority on cytotoxicity against free drug exposure.

3.2. IN VIVO EXPERIMENTS

3.2.1. In Vivo Localization

To illustrate targeting ability of aptamer-based nanovalve system in vivo, allograft murine breast cancer model was used. As soon as tumor volume reached palpable size (150mm^3), tumor bearing mouse was injected with Apta-NP-Fl complex subcutaneously and in vivo fluorescence image was acquired with one-hour interval after injection. As shown in Figure 3.12, fluorescent signal localizes around tumor region after one hour of injection as aptamer-based nanovalve system aims. And intensity increases up to four hours after injection. Fluorescent signal around tumor region shows localized drug release around tumor. After 24 hours fluorescence amount decreases around tumor.

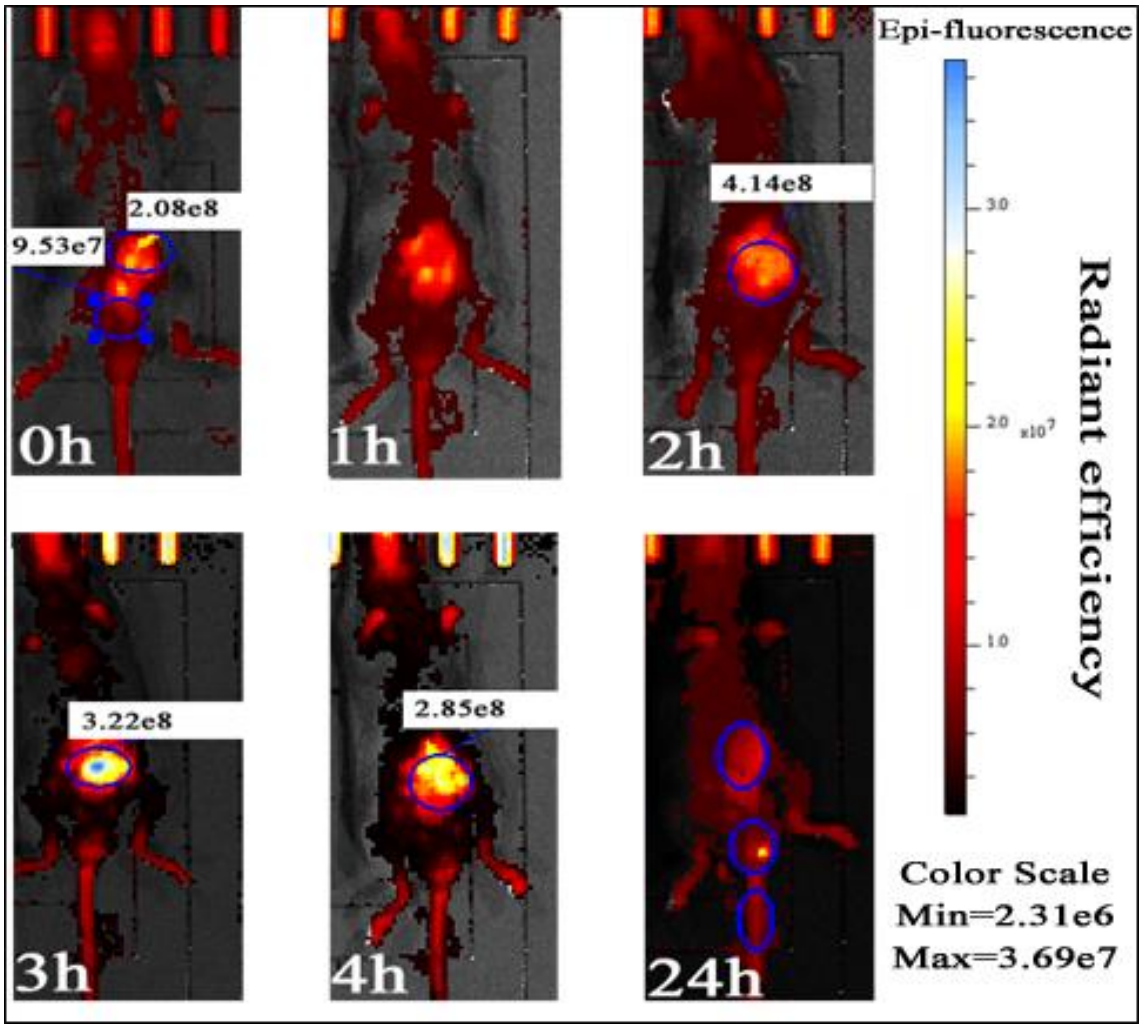

Figure 3.12. In vivo localization of Apta-NP complex around tumor region. Fluorescence image was acquired with one-hour interval after subcutaneous Apta-NP-Fl injection was made.

4. DISCUSSION

Chemotherapeutic agents used in clinics for breast cancer therapy like doxorubicin and paclitaxel are given intravenously as free drugs, without any targeted delivery system. Chemotherapeutic drugs have different mechanisms of actions, such as; doxorubicin inhibit topoisomerase activity while paclitaxel stabilizes formed microtubule structure [28, 29, 48]. However, they lack the ability to specifically target tumor tissue. Due to incapability of those drugs to specifically target tumor tissue, drugs accumulate on vital organs like brain and hearth after they enter systemic circulation as reported in previous studies [36, 58]. Accumulation of those drugs on those organs causes systemic toxicity. Because of that reason, systemic toxicity is one of the dose limiting factors for current chemotherapeutic agents [42, 58, 59, 231]. Furthermore, using traditional chemotherapeutic agents yield less than 50 per cent complete response rate [232, 233]. To increase efficacy of drugs, targeted delivery strategies recruiting nanoparticles have been studied which also aims to decrease drug induced systemic toxicity. [174] In addition to those, patients develop drug resistance to routinely used chemotherapeutic agents in breast cancer [52]. Even though drug is delivered to the target tissue, high amount of release may induce drug resistance against the given drug [57, 234].

Aptamers are single stranded DNA or RNA oligonucleotides which have high affinity and specificity against their targets. Because of their superior properties against monoclonal antibodies, aptamers are vastly studied as targeting agents or chemotherapeutic agents as themselves. [97, 98]

To address both issues caused by inefficiency of chemotherapeutic agents used in clinics, targeted delivery approaches have been used [64]. Many different approaches such as liposomes [181], dendrimers [185] and polymeric nanoparticles [184]; silica nanoparticles are one of most intensely studied delivery vehicles due to their advantages such as high surface area/ volume ratio, structured pores, modification of silanol surface [206, 207]. In this research, we used nucleolin targeting aptamer functionalized MCM-41 type silica nanoparticles. Capping of MCM-41 type silica nanoparticles provided aptamer nanovalve capability to the drug delivery system which aimed to overcome both drug resistance and low efficacy of current therapeutic approaches.

Uptake, localization, and cytotoxic effect of chemotherapeutic agent loaded aptamer gated drug delivery system was studied for its on in vitro and in vivo breast cancer models in this research.

Characterization of MCM-41 type silica nanoparticle has been made by SEM, TEM and AFM imaging. TEM imaging showed typical hexagonal nanopores of MCM-41 type material [228, 229, 235] as SEM imaging showed typical aggregated, spherical, round nanoparticles as shown in Figure 3.1, 3.2 and 3.3 [228, 229, 236]. Maximum height of particles was ranging from 20-200 μm and average hydrodynamic diameter of nanoparticles were measured as 191± 1.3nm by DLS [228, 229] as seen in Figure 3.4. Specific peaks providing information about amino functionalization on nanoparticles were shown on FTIR spectra, specifically peaks on 1460 nm and 690 nm shows N-H asymmetric bending vibrations and N-H bending respectively as shown in Figure 3.5 [228-230].

To determine increased uptake of fluorescein into cells, Apta-NP-Fl drug delivery complex was used on E0771 cells. Previously, increased uptake of fluorescein by Apta-NP-Fl was shown in comparison to NP-Fl on nucleolin positive MDA-MB 231 cells [227]. Current study showed similar fashion on nucleolin positive E0771 cells. Percentage of fluorescein stained population of Apta-NP-Fl treated cells were two-fold of the percentage of fluorescein stained population of NP-Fl treated cells for all doses. In the current study, AS1411 aptamers were used to cap pores of mesoporous silica nanoparticles. Studies showed that, uptake of fluorescein cargo into cells can be increased by surface modifications of MCM-41 type silica nanoparticles [214]. Moreover, even though exact mechanism is still being researched, nucleolin mediated uptake of AS1411 aptamer has been shown on nucleolin positive cells [165]. Thus, further modifications on surface of silica nanoparticle may affect uptake. In addition to those, cancer cells engulf nanoparticles via endocytosis [237]. Although, higher uptake of fluorescein cargo was observed on Apta-NP-Fl treated cells, properties of cancer cells to engulf nanoparticles might be the cause of increasing uptake of fluorescein cargo of NP-Fl.

Following flow cytometry experiments, we examined cellular uptake of fluorescein by fluorescence microscopy. Supporting flow cytometry analysis, intense fluorescence around nucleus of cells was also observed on E0771 cells treated with Apta-NP-Fl while weak signal obtained from cells treated with NP-Fl. Those results are parallel to the previously published

similar constructs in which ability of Apta-NP delivery complex to target only nucleolin positive cells has been shown [227].

After completion of internalization and uptake experiment, we have examined effect of Apt-NP-TXL usage on E0771 murine breast cancer cell viability to validate previous experiments. Silica nanoparticles by themselves did not show significant toxicity against E0771 cells (Figure 3.10) ($p>0.05$). However, increased cytotoxicity was shown on dose dependent manner on cells treated with Apta-NP-TXL in comparison to free TXL. While 24 hours of Apta-NP-TXL treatment showed significant cytotoxicity in comparison to control group starting from 2.5 µM, 24 hours of free TXL treatment showed significant cytotoxicity starting from 50 µM. Even though higher cytotoxicity has been shown for both drugs for 48 hours treatment, Apt-NP-TXL delivery system shows lower IC50 value still in comparison to free paclitaxel group.

In vivo localization of Apta-NP complex was examined by injection of fluorescein loaded Apta-NP subcutaneously to E0771 allograft tumor bearing C57bl/6 mouse. After one hour from injection, rapid localization of nanoparticles around tumor was observed by increased fluorescence intensity while fluorescence on other regions was not visible. After 24 hours from injection, fluorescence intensity decreased, and it may be due to removal of drug from the system since fluorescence signal was obtained from the end of rectum.

Even though statistical significance could not be obtained from in vitro cytotoxicity experiments, better targeting and increased uptake of the cargo of aptamer gated drug delivery system has been shown. This property might be used to decrease side effects of chemotherapeutic agents on healthy tissue and also to overcome drug resistance.

5. CONCLUSION

In this study, firstly, Apta-NP drug delivery system was characterized by SEM, TEM and AFM microscopy, DLS and FTIR. Then, ability of fluorescein loaded Apta-NP complex to target nucleolin positive breast cancer cell and increased uptake of fluorescein in comparison to NP-Fl has been shown similar to the previous studies by both flow cytometry analysis and fluorescence microscopy [227]. On flow cytometry analysis, fluorescein stained cell population on fluorescein loaded Apta-NP treated group was two-fold fluorescein stained cell population of fluorescein loaded NP treated group. Following that, fluorescence microscopy was applied to validate flow cytometry results and also localization of fluorescein around nucleus was detected for Apta-NP-Fl treated cells, while low fluorescence signal was obtained from NP-Fl treated group.

Following characterization experiments, cytotoxic effect of chemotherapeutic drug carrying Apta-NP drug delivery system was shown **for the first time**. Paclitaxel carrying Apta-NP complex showed increased cytotoxicity on nucleolin positive breast cancer cells in comparison to free paclitaxel. IC50 values for Apta-NP-TXL and free TXL were 45.76 µM and 36.41 µM for 24 hours of treatment respectively while IC50 values for same drugs were 48.87 µM and 35.64 µM for 48 hours of treatment respectively.

Apta-NP complex is also able to target breast cancer tissue on developed allograft mouse breast cancer model with same breast cancer cell line as shown in this study **for the first time**. One hour after subcutaneous injection on allograft breast tumor carrying mice, localization of fluorescence signal around breast tumor has been shown.

To conclude, advantages of using aptamer gated targeted drug delivery systems over free drug and/or non-targeted delivery systems on uptake, localization, and cytotoxicity has been shown in both in vitro and in vivo systems. Therefore, aptamer gated drug delivery system used in this study might be used for breast cancer diagnosis and therapeutics. Further studies are required for confirmation of results on other cell lines and chemotherapeutic drugs.

6. FUTURE DIRECTIONS

Although IC50 value obtained from paclitaxel loaded Apta-NP treatment is already lower than IC50 value of free paclitaxel treatment for both 24 hours and 48 hours of exposure, drug delivery system should be improved for higher efficacy. Surface modifications on silica nanoparticles might be useful method for such improvement.

Following this study, we would like to recruit more chemotherapeutic agents as cargo of the Apta-NP drug delivery system, such as doxorubicin. Chemotherapeutic agents have different mechanisms of actions and we would like to use the most compatible drug with the Apta-NP drug delivery system for further research.

Then, in parallel to that, we will show the cytotoxic effect and penetration capability of drug or fluorescein loaded Apta-NP delivery system on 3D spheroid culture in comparison to free drug. Following that, similar experiments should be repeated on other murine and human breast cancer lines such as 4T1, MCF-7 and MDA-MB-231.

Finally, effect of Apta-NP drug delivery system on treatment of breast cancer on allograft or xenograft mouse breast cancer models with chemotherapeutic drug loaded Apta-NP complex will be studied. During this experiment, effect of free drug and aptamer gated drug delivery system on healthy tissue, distribution on vital organs will be determined.

REFERENCES

1. Ozmen V, Dagoglu N, Dede I, Akcakaya A, Kerem M, Goksel F, et al. Turkish ministry of health, 2(nd) Turkish medical general assembly clinical oncology study group report. *European Journal of Breast Health*. 2016;12(1):9-17.

2. Fidler MM, Gupta S, Soerjomataram I, Ferlay J, Steliarova-Foucher E, Bray F. Cancer incidence and mortality among young adults aged 20-39 years worldwide in 2012: A population-based study. *The Lancet Oncology*. 2017;18(12):1579-89.

3. Ozmen V, Ozcinar B, Karanlik H, Cabioglu N, Tukenmez M, Disci R, et al. Breast cancer risk factors in turkish women--a university hospital based nested case control study. *World Journal of Surgical Oncology*. 2009;7:37-45.

4. Ozmen V. Breast cancer in Turkey: Clinical and histopathological characteristics (analysis of 13.240 patients). *European Journal of Breast Health*. 2014;10(2):98-105.

5. Dogan N, Toprak D. Female breast cancer mortality rates in Turkey. *Asian Pacific Journal of Cancer Prevention*. 2014;15(18):7569-73.

6. Siegel RL, Miller KD, Jemal A. Cancer statistics, 2018. *A Cancer Journal for Clinicians*. 2018;68(1):7-30.

7. Siegel RL, Miller KD, Jemal A. Cancer statistics, 2017. *A Cancer Journal for Clinicians*. 2017;67(1):7-30.

8. DeSantis CE, Ma J, Goding Sauer A, Newman LA, Jemal A. Breast cancer statistics, 2017, racial disparity in mortality by state. *A Cancer Journal for Clinicians*. 2017;67(6):439-48.

9. Malhotra GK, Zhao X, Band H, Band V. Histological, molecular and functional subtypes of breast cancers. *Cancer Biology & Therapy*. 2010;10(10):955-60.

10. Elston CW. Classification and grading of invasive breast carcinoma. *Verhandlungen der Deutschen Gesellschaft für Pathologie*. 2005;89:35-44.

11. Rakha EA, Reis-Filho JS, Baehner F, Dabbs DJ, Decker T, Eusebi V, et al. Breast cancer prognostic classification in the molecular era: The role of histological grade. *Breast Cancer Research*. 2010;12(4):207-219.

12. Makki J. Diversity of breast carcinoma: Histological subtypes and clinical relevance. *Clinical Medicine Insights: Pathology*. 2015;8:23-31.

13. Whitman GJ, Sheppard DG, Phelps MJ, Gonzales BN. Breast cancer staging. *Seminars in Roentgenology*. 2006;41(2):91-104.

14. Perou CM, Sorlie T, Eisen MB, van de Rijn M, Jeffrey SS, Rees CA, et al. Molecular portraits of human breast tumours. *Nature*. 2000;406(6797):747-52.

15. Dai X, Li T, Bai Z, Yang Y, Liu X, Zhan J, et al. Breast cancer intrinsic subtype classification, clinical use and future trends. *American Journal of Cancer Research*. 2015;5(10):2929-43.

16. Goldhirsch A, Wood WC, Coates AS, Gelber RD, Thurlimann B, Senn HJ, et al. Strategies for subtypes--dealing with the diversity of breast cancer: Highlights of the st. Gallen international expert consensus on the primary therapy of early breast cancer 2011. *Annals of Oncology*. 2011;22(8):1736-47.

17. Hennigs A, Riedel F, Gondos A, Sinn P, Schirmacher P, Marme F, et al. Prognosis of breast cancer molecular subtypes in routine clinical care: A large prospective cohort study. *BMC Cancer*. 2016;16(1):734-743.

18. Koboldt DC, Fulton RS, McLellan MD, Schmidt H, Kalicki-Veizer J, McMichael JF Comprehensive molecular portraits of human breast tumours. *Nature*. 2012;490(7418):61-70.

19. Prat A, Perou CM. Deconstructing the molecular portraits of breast cancer. *Molecular Oncology*. 2011;5(1):5-23.

20. Fallahpour S, Navaneelan T, De P, Borgo A. Breast cancer survival by molecular subtype: A population-based analysis of cancer registry data. *Canadian Medical Association Journal*. 2017;5(3):E734-E9.

21. Pracht M, Berthold D. Successes and limitations of targeted therapies in renal cell carcinoma. *Progress in Tumor Research*. 2014;41:98-112.

22. Curigliano G, Criscitiello C. Successes and limitations of targeted cancer therapy in breast cancer. *Progress in Tumor Research*. 2014;41:15-35.

23. Shahriari-Ahmadi A, Arabi M, Payandeh M, Sadeghi M. The recurrence frequency of breast cancer and its prognostic factors in Iranian patients. *International Journal of Applied and Basic Medical Research*. 2017;7(1):40-3.

24. Rostas JW, Dyess DL. Current operative management of breast cancer: An age of smaller resections and bigger cures. *International Journal of Breast Cancer*. 2012;2012:516417-24.

25. Nicholson RI, Johnston SR. Endocrine therapy--current benefits and limitations. *Breast Cancer Research and Treatment*. 2005;93 Suppl 1:S3-10.

26. Thompson A, Brennan K, Cox A, Gee J, Harcourt D, Harris A, et al. Evaluation of the current knowledge limitations in breast cancer research: A gap analysis. *Breast Cancer Research*. 2008;10(2):R26.

27. Wani MC, Horwitz SB. Nature as a remarkable chemist: A personal story of the discovery and development of taxol. *Anticancer Drugs*. 2014;25(5):482-7.

28. Weaver BA. How taxol/paclitaxel kills cancer cells. *Molecular Biology of the Cell*. 2014;25(18):2677-81.

29. Horwitz SB. Taxol (paclitaxel): Mechanisms of action. *Annals of Oncology*. 1994;5 Suppl 6:S3-6.

30. Nogales E. Structural insights into microtubule function. *Annual Review of Biochemistry*. 2000;69:277-302.

31. Itoh TJ, Hotani H. Microtubule dynamics and the regulation by microtubule-associated proteins (maps). *Biological Sciences in Space*. 2004;18(3):116-7.

32. Robinson D, Beattie P, Sherwin T, Gull K. Microtubules, tubulin, and microtubule-associated proteins of trypanosomes. *Methods in Enzymology*. 1991;196:285-99.

33. Schiff PB, Horwitz SB. Taxol stabilizes microtubules in mouse fibroblast cells. *Proceedings of the National Academy of Sciences of the United States of America*. 1980;77(3):1561-5.

34. Schiff PB, Fant J, Horwitz SB. Promotion of microtubule assembly in vitro by taxol. *Nature*. 1979;277(5698):665-7.

35. Ateba SB, Ngeu ST, Mvondo MA, Tchoumtchoua J, Awounfack CF, Krenn L. Natural terpenoids against female breast cancer: A 5-year recent research. *Current Medicinal Chemistry*. 2018;25(27):3162-3213.

36. Scripture CD, Figg WD, Sparreboom A. Peripheral neuropathy induced by paclitaxel: Recent insights and future perspectives. *Current Neuropharmacology*. 2006;4(2):165-72.

37. Postma TJ, Vermorken JB, Liefting AJ, Pinedo HM, Heimans JJ. Paclitaxel-induced neuropathy. *Annals of Oncology*. 1995;6(5):489-94.

38. Lichtman SM, Hurria A, Cirrincione CT, Seidman AD, Winer E, Hudis C, et al. Paclitaxel efficacy and toxicity in older women with metastatic breast cancer: Combined analysis of calgb 9342 and 9840. *Annals of Oncology*. 2012;23(3):632-8.

39. Rowinsky EK, Donehower RC. Paclitaxel (taxol). *The New England Journal of Medicine*. 1995;332(15):1004-14.

40. Gadducci A, Gargini A, Palla E, Fanucchi A, Genazzani AR. Neutropenic enterocolitis in an advanced epithelial ovarian cancer patient treated with paclitaxel/platinum-based chemotherapy: A case report and review of the literature. *Anticancer Research*. 2005;25(3c):2509-13.

41. Eisenhauer EA, ten Bokkel Huinink WW, Swenerton KD, Gianni L, Myles J, van der Burg ME, et al. European-canadian randomized trial of paclitaxel in relapsed ovarian cancer: High-dose versus low-dose and long versus short infusion. *Journal of Clinical Oncology* 1994;12(12):2654-66.

42. Marupudi NI, Han JE, Li KW, Renard VM, Tyler BM, Brem H. Paclitaxel: A review of adverse toxicities and novel delivery strategies. *Expert Opinion on Drug Safety*. 2007;6(5):609-21.

43. Vasantha J, Kannan G, Goud T, Palani T, Vanitha R, Anitha R, et al. Pharmacokinetic evaluation of paclitaxel in south indian cancer patients: A prospective study. *Journal of Young Pharmacists*. 2011;3(4):322-8.

44. Ohtsu T, Sasaki Y, Tamura T, Miyata Y, Nakanomyo H, Nishiwaki Y, et al. Clinical pharmacokinetics and pharmacodynamics of paclitaxel: A 3-hour infusion versus a 24-hour infusion. *Clinical Cancer Research*. 1995;1(6):599-606.

45. Qi N, Li F, Li X, Kang H, Zhao H, Du N. Combination use of paclitaxel and avastin enhances treatment effect for the NSCLC patients with malignant pleural effusion. *Medicine (Baltimore)*. 2016;95(47):e5392.

46. Senapati S, Mahanta AK, Kumar S, Maiti P. Controlled drug delivery vehicles for cancer treatment and their performance. *Signal Transduction and Targeted Therapy*. 2018;3:7-26.

47. Patel AG, Kaufmann SH. How does doxorubicin work? *Elife*. 2012;1:e00387.

48. Tewey KM, Rowe TC, Yang L, Halligan BD, Liu LF. Adriamycin-induced DNA damage mediated by mammalian DNA topoisomerase II. *Science*. 1984;226(4673):466-8.

49. Champoux JJ. DNA topoisomerases: Structure, function, and mechanism. *Annual Review of Biochemistry*. 2001;70:369-413.

50. Pilco-Ferreto N, Calaf GM. Influence of doxorubicin on apoptosis and oxidative stress in breast cancer cell lines. *International Journal of Oncology*. 2016;49(2):753-62.

51. Pawlowska J, Tarasiuk J, Wolf CR, Paine MJ, Borowski E. Differential ability of cytostatics from anthraquinone group to generate free radicals in three enzymatic systems: NADH dehydrogenase, NADPH cytochrome p450 reductase, and xanthine oxidase. *Oncology Research and Treatment*. 2003;13(5):245-52.

52. Gonzalez-Angulo AM, Morales-Vasquez F, Hortobagyi GN. Overview of resistance to systemic therapy in patients with breast cancer. *Advances in Experimental Medicine and Biology*. 2007;608:1-22.

53. Cortazar P, Justice R, Johnson J, Sridhara R, Keegan P, Pazdur R. Us food and drug administration approval overview in metastatic breast cancer. *Journal of Clinical Oncology*. 2012;30(14):1705-11.

54. Kaye S, Merry S. Tumour cell resistance to anthracyclines--a review. *Cancer Chemotherapy and Pharmacology*. 1985;14(2):96-103.

55. Thorn CF, Oshiro C, Marsh S, Hernandez-Boussard T, McLeod H, Klein TE, et al. Doxorubicin pathways: Pharmacodynamics and adverse effects. *Pharmacogenet Genomics*. 2011;21(7):440-6.

56. Sarkadi B, Homolya L, Szakacs G, Varadi A. Human multidrug resistance ABCb and ABCg transporters: Participation in a chemoimmunity defense system. *Physiological Reviews*. 2006;86(4):1179-236.

57. Kibria G, Hatakeyama H, Akiyama K, Hida K, Harashima H. Comparative study of the sensitivities of cancer cells to doxorubicin, and relationships between the effect of the drug-efflux pump p-gp. *Biological and Pharmaceutical Bulletin*. 2014;37(12):1926-35.

58. Volkova M, Russell R, 3rd. Anthracycline cardiotoxicity: Prevalence, pathogenesis and treatment. *Current Cardiology Reviews*. 2011;7(4):214-20.

59. Swain SM, Whaley FS, Ewer MS. Congestive heart failure in patients treated with doxorubicin: A retrospective analysis of three trials. *Cancer*. 2003;97(11):2869-79.

60. Von Hoff DD, Layard MW, Basa P, Davis HL, Jr., Von Hoff AL, Rozencweig M, et al. Risk factors for doxorubicin-induced congestive heart failure. *Annals of Internal Medicine*. 1979;91(5):710-7.

61. Wu R, Wang HL, Yu HL, Cui XH, Xu MT, Xu X, et al. Doxorubicin toxicity changes myocardial energy metabolism in rats. *Chemico-Biological Interactions*. 2016;244:149-58.

62. Beck PL, Wong JF, Li Y, Swaminathan S, Xavier RJ, Devaney KL, et al. Chemotherapy- and radiotherapy-induced intestinal damage is regulated by intestinal trefoil factor. *Gastroenterology*. 2004;126(3):796-808.

63. Bhatnagar B, Gilmore S, Goloubeva O, Pelser C, Medeiros M, Chumsri S, et al. Chemotherapy dose reduction due to chemotherapy induced peripheral neuropathy in breast cancer patients receiving chemotherapy in the neoadjuvant or adjuvant settings: A single-center experience. *Springerplus*. 2014;3:366-72.

64. Masoud V, Pages G. Targeted therapies in breast cancer: New challenges to fight against resistance. *World Journal of Clinical Oncology*. 2017;8(2):120-34.

65. Liu M, Yu X, Chen Z, Yang T, Yang D, Liu Q, et al. Aptamer selection and applications for breast cancer diagnostics and therapy. *Journal of Nanobiotechnology*. 2017;15(1):81-97.

66. Zhou G, Wilson G, Hebbard L, Duan W, Liddle C, George J, et al. Aptamers: A promising chemical antibody for cancer therapy. *Oncotarget*. 2016;7(12):13446-63.

67. Sun H, Zhu X, Lu PY, Rosato RR, Tan W, Zu Y. Oligonucleotide aptamers: New tools for targeted cancer therapy. *Molecular Therapy - Nucleic Acids*. 2014;3:e182.

68. Zhang X, Soori G, Dobleman TJ, Xiao GG. The application of monoclonal antibodies in cancer diagnosis. *Expert Review of Molecular Diagnostics*. 2014;14(1):97-106.

69. Kohler G, Milstein C. Continuous cultures of fused cells secreting antibody of predefined specificity. *Nature*. 1975;256(5517):495-7.

70. Chames P, Van Regenmortel M, Weiss E, Baty D. Therapeutic antibodies: Successes, limitations and hopes for the future. *British Journal of Pharmacology*. 2009;157(2):220-33.

71. Little M, Kipriyanov SM, Le Gall F, Moldenhauer G. Of mice and men: Hybridoma and recombinant antibodies. *Immunology Today*. 2000;21(8):364-70.

72. Liu JK. The history of monoclonal antibody development - progress, remaining challenges and future innovations. *Annals of Medicine and Surgery*. 2014;3(4):113-6.

73. Chung J. Special issue on therapeutic antibodies and biopharmaceuticals. *Experimental & Molecular Medicine*. 2017;49(3):e304.

74. Boekhout AH, Beijnen JH, Schellens JH. Trastuzumab. *Oncologist*. 2011;16(6):800-10.

75. Vu T, Claret FX. Trastuzumab: Updated mechanisms of action and resistance in breast cancer. *Frontiers in Oncology*. 2012;2:62-8.

76. Slamon DJ, Leyland-Jones B, Shak S, Fuchs H, Paton V, Bajamonde A, et al. Use of chemotherapy plus a monoclonal antibody against HER2 for metastatic breast cancer that overexpresses HER2. *The New England Journal of Medicine*. 2001;344(11):783-92.

77. Lan KH, Lu CH, Yu D. Mechanisms of trastuzumab resistance and their clinical implications. *Annals of the New York Academy of Sciences*. 2005;1059:70-5.

78. Gajria D, Chandarlapaty S. Her2-amplified breast cancer: Mechanisms of trastuzumab resistance and novel targeted therapies. *Expert Review of Anticancer Therapy*. 2011;11(2):263-75.

79. van Hasselt JG, Boekhout AH, Beijnen JH, Schellens JH, Huitema AD. Population pharmacokinetic-pharmacodynamic analysis of trastuzumab-associated cardiotoxicity. *Clinical Pharmacology & Therapeutics*. 2011;90(1):126-32.

80. Fay F, Scott CJ. Antibody-targeted nanoparticles for cancer therapy. *Immunotherapy*. 2011;3(3):381-94.

81. Cirstoiu-Hapca A, Buchegger F, Lange N, Bossy L, Gurny R, Delie F. Benefit of anti-HER2-coated paclitaxel-loaded immuno-nanoparticles in the treatment of disseminated ovarian cancer: Therapeutic efficacy and biodistribution in mice. *Journal of Controlled Release*. 2010;144(3):324-31.

82. Cirstoiu-Hapca A, Bossy-Nobs L, Buchegger F, Gurny R, Delie F. Differential tumor cell targeting of anti-HER2 (herceptin) and anti-CD20 (mabthera) coupled nanoparticles. *International Journal of Pharmaceutics*. 2007;331(2):190-6.

83. Jiang W, Kim BY, Rutka JT, Chan WC. Nanoparticle-mediated cellular response is size-dependent. *Nature Nanotechnology*. 2008;3(3):145-50.

84. Tuerk C, Gold L. Systematic evolution of ligands by exponential enrichment: RNA ligands to bacteriophage T4 DNA polymerase. *Science*. 1990;249(4968):505-10.

85. Ellington AD, Szostak JW. In vitro selection of RNA molecules that bind specific ligands. *Nature*. 1990;346(6287):818-22.

86. Zhou J, Rossi J. Aptamers as targeted therapeutics: Current potential and challenges. *Nature Reviews Drug Discovery*. 2017;16(3):181-202.

87. Gragoudas ES, Adamis AP, Cunningham ET, Jr., Feinsod M, Guyer DR, Group VISiONCT. Pegaptanib for neovascular age-related macular degeneration. *The New England Journal of Medicine*. 2004;351(27):2805-16.

88. Lim LS, Mitchell P, Seddon JM, Holz FG, Wong TY. Age-related macular degeneration. *The Lancet*. 2012;379(9827):1728-38.

89. Tobin KA. Macugen treatment for wet age-related macular degeneration. *Insight*. 2006;31(1):11-4.

90. Ishibashi T. Long-term efficacy and safety profile of pegaptanib sodium for age-related macular degeneration with choroidal neovascularization--evaluation of extended phase ii clinical trial. *Nippon Ganka Gakkai Zasshi*. 2011;115(2):122-33.

91. Rosina C, Bottoni F, Staurenghi G. Clinical experience with pegaptanib sodium. *Clinical Ophthalmology*. 2008;2(3):485-8.

92. Ruggeri ZM. The role of von willebrand factor in thrombus formation. *Thrombosis Research*. 2007;120 Suppl 1:S5-9.

93. Sadler JE. Biochemistry and genetics of Von Willebrand Factor. *Annual Review of Biochemistry*. 1998;67:395-424.

94. Spiel AO, Mayr FB, Ladani N, Wagner PG, Schaub RG, Gilbert JC, et al. The aptamer arc1779 is a potent and specific inhibitor of von willebrand factor mediated ex vivo platelet function in acute myocardial infarction. *Platelets*. 2009;20(5):334-40.

95. Denorme F, De Meyer SF. The vwf-gpib axis in ischaemic stroke: Lessons from animal models. *Thrombosis and Haemostasis*. 2016;116(4):597-604.

96. Cosmi B. Arc-1779, a pegylated aptamer antagonist of von willebrand factor for potential use as an anticoagulant or antithrombotic agent. *Current opinion in molecular therapeutics*. 2009;11(3):322-8.

97. Parashar A. Aptamers in therapeutics. *Journal of Clinical and Diagnostic Research*. 2016;10(6):BE01-6.

98. Ozalp VC, Kavruk M, Dilek O, Bayrac AT. Aptamers: Molecular tools for medical diagnosis. *Current Topics in Medicinal Chemistry*. 2015;15(12):1125-37.

99. Wu X, Shaikh AB, Yu Y, Li Y, Ni S, Lu A, et al. Potential diagnostic and therapeutic applications of oligonucleotide aptamers in breast cancer. *International Journal of Molecular Sciences*. 2017;18(9):1851-74.

100. Sun X, Cheng G, Hao M, Zheng J, Zhou X, Zhang J, et al. CXCL12 / CXCR4 / CXCR7 chemokine axis and cancer progression. *Cancer and Metastasis Reviews*. 2010;29(4):709-22.

101. Guo F, Wang Y, Liu J, Mok SC, Xue F, Zhang W. Cxcl12/cxcr4: A symbiotic bridge linking cancer cells and their stromal neighbors in oncogenic communication networks. *Oncogene*. 2016;35(7):816-26.

102. Marasca R, Maffei R. NOX-a12: Mobilizing CLL away from home. *Blood*. 2014;123(7):952-3.

103. Burger JA, Tsukada N, Burger M, Zvaifler NJ, Dell'Aquila M, Kipps TJ. Blood-derived nurse-like cells protect chronic lymphocytic leukemia b cells from spontaneous apoptosis through stromal cell-derived factor-1. *Blood*. 2000;96(8):2655-63.

104. Kurtova AV, Balakrishnan K, Chen R, Ding W, Schnabl S, Quiroga MP, et al. Diverse marrow stromal cells protect cll cells from spontaneous and drug-induced apoptosis: Development of a reliable and reproducible system to assess stromal cell adhesion-mediated drug resistance. *Blood*. 2009;114(20):4441-50.

105. Song KM, Lee S, Ban C. Aptamers and their biological applications. *Sensors (Basel)*. 2012;12(1):612-31.

106. Shi J, Lyu J, Tian F, Yang M. A fluorescence turn-on biosensor based on graphene quantum dots (GQDS) and molybdenum disulfide (MOS2) nanosheets for epithelial cell adhesion molecule (EpCAM) detection. *Biosensors and Bioelectronics*. 2017;93:182-8.

107. Mi J, Ray P, Liu J, Kuan CT, Xu J, Hsu D, et al. In vivo selection against human colorectal cancer xenografts identifies an aptamer that targets rna helicase protein dhx9. *Molecular Therapy - Nucleic Acids*. 2016;5:e315.

108. Niazi JH, Verma SK, Niazi S, Qureshi A. In vitro HER2 protein-induced affinity dissociation of carbon nanotube-wrapped anti- HER2 aptamers for HER2 protein detection. *Analyst*. 2015;140(1):243-9.

109. Li H, Bai X, Wang N, Chen X, Li J, Zhang Z, et al. Aptamer-based microcantilever biosensor for ultrasensitive detection of tumor marker nucleolin. *Talanta*. 2016;146:727-31.

110. Jo H, Gu H, Jeon W, Youn H, Her J, Kim SK, et al. Electrochemical aptasensor of cardiac troponin I for the early diagnosis of acute myocardial infarction. *Analytical Chemistry*. 2015;87(19):9869-75.

111. Tombelli S, Minunni M, Luzi E, Mascini M. Aptamer-based biosensors for the detection of HIV-1 tat protein. *Bioelectrochemistry*. 2005;67(2):135-41.

112. Famulok M, Mayer G. Aptamers and selex in chemistry & biology. *Chemistry & Biology*. 2014;21(9):1055-8.

113. Ding F, Gao Y, He X. Recent progresses in biomedical applications of aptamer-functionalized systems. *Bioorganic & Medicinal Chemistry Letters*. 2017;27(18):4256-69.

114. Meng HM, Liu H, Kuai H, Peng R, Mo L, Zhang XB. Aptamer-integrated DNA nanostructures for biosensing, bioimaging and cancer therapy. *Chemical Engineering Science*. 2016;45(9):2583-602.

115. Dong Y, Xu Y, Yong W, Chu X, Wang D. Aptamer and its potential applications for food safety. *Critical Reviews in Food Science and Nutrition*. 2014;54(12):1548-61.

116. Bayrac C, Eyidogan F, Avni Oktem H. DNA aptamer-based colorimetric detection platform for salmonella enteritidis. *Biosensors and Bioelectronics*. 2017;98:22-8.

117. Ilgu M, Nilsen-Hamilton M. Aptamers in analytics. *Analyst*. 2016;141(5):1551-68.

118. Xu Y, Han T, Li X, Sun L, Zhang Y, Zhang Y. Colorimetric detection of kanamycin based on analyte-protected silver nanoparticles and aptamer-selective sensing mechanism. *Analytica Chimica Acta*. 2015;891:298-303.

119. Chen XJ, Huang YK, Ma XY, Jia F, Guo XF, Wang ZP. Impedimetric aptamer-based determination of the mold toxin fumonisin b1. *Microchimica Acta*. 2015;182(9-10):1709-14.

120. Mejri-Omrani N, Miodek A, Zribi B, Marrakchi M, Hamdi M, Marty JL, et al. Direct detection of ota by impedimetric aptasensor based on modified polypyrrole-dendrimers. *Analytica Chimica Acta*. 2016;920:37-46.

121. Rapini R, Marrazza G. Electrochemical aptasensors for contaminants detection in food and environment: Recent advances. *Bioelectrochemistry*. 2017;118:47-61.

122. Stoltenburg R, Reinemann C, Strehlitz B. Selex--a (r)evolutionary method to generate high-affinity nucleic acid ligands. *Biomolecular Engineering*. 2007;24(4):381-403.

123. Zhuo Z, Yu Y, Wang M, Li J, Zhang Z, Liu J, et al. Recent advances in selex technology and aptamer applications in biomedicine. *International Journal of Molecular Sciences*. 2017;18(10):2142-61.

124. Gopinath SC. Methods developed for SELEX. *Analytical and Bioanalytical Chemistry*. 2007;387(1):171-82.

125. Lee JF, Stovall GM, Ellington AD. Aptamer therapeutics advance. *Current Opinion in Chemical Biology*. 2006;10(3):282-9.

126. Kopylov AM, Spiridonova VA. Combinatorial chemistry of nucleic acids: SELEX. *Molecular Biology*. 2000;34(6):1097-113.

127. Ohuchi S. Cell-SELEX technology. *BioResearch Open Access*. 2012;1(6):265-72.

128. Chen M, Yu Y, Jiang F, Zhou J, Li Y, Liang C, et al. Development of cell-SELEX technology and its application in cancer diagnosis and therapy. *International Journal of Molecular Sciences*. 2016;17(12):2079-91.

129. Cheng C, Chen YH, Lennox KA, Behlke MA, Davidson BL. In vivo SELEX for identification of brain-penetrating aptamers. *Molecular Therapy - Nucleic Acids*. 2013;2:e67.

130. Sundaram P, Kurniawan H, Byrne ME, Wower J. Therapeutic RNA aptamers in clinical trials. *European Journal of Pharmaceutical Sciences*. 2013;48(1-2):259-71.

131. Stein CA, Castanotto D. FDA-approved oligonucleotide therapies in 2017. *Molecular Therapy*. 2017;25(5):1069-75.

132. Catuogno S, Esposito CL. Aptamer cell-based selection: Overview and advances. *Biomedicines*. 2017;5(3):49-67.

133. Thiviyanathan V, Gorenstein DG. Aptamers and the next generation of diagnostic reagents. *Proteomics Clinical Applications*. 2012;6(11-12):563-73.

134. Chen A, Yang S. Replacing antibodies with aptamers in lateral flow immunoassay. *Biosensors and Bioelectronics*. 2015;71:230-42.

135. Zhu G, Niu G, Chen X. Aptamer-drug conjugates. *Bioconjugate Chemistry*. 2015;26(11):2186-97.

136. Ni S, Yao H, Wang L, Lu J, Jiang F, Lu A, et al. Chemical modifications of nucleic acid aptamers for therapeutic purposes. *International Journal of Molecular Sciences*. 2017;18(8):1683-704.

137. Lakhin AV, Tarantul VZ, Gening LV. Aptamers: Problems, solutions and prospects. *Acta Naturae*. 2013;5(4):34-43.

138. Birch JR, Racher AJ. Antibody production. *Advanced Drug Delivery Reviews*. 2006;58(5-6):671-85.

139. Jayasena SD. Aptamers: An emerging class of molecules that rival antibodies in diagnostics. *Clinical Chemistry*. 1999;45(9):1628-50.

140. Burge S, Parkinson GN, Hazel P, Todd AK, Neidle S. Quadruplex DNA: Sequence, topology and structure. *Nucleic Acids Research*. 2006;34(19):5402-15.

141. Bates PJ, Reyes-Reyes EM, Malik MT, Murphy EM, O'Toole MG, Trent JO. G-quadruplex oligonucleotide as1411 as a cancer-targeting agent: Uses and mechanisms. *Biochimica et Biophysica Acta*. 2017;1861(5 Pt B):1414-28.

142. Choi EW, Nayak LV, Bates PJ. Cancer-selective antiproliferative activity is a general property of some g-rich oligodeoxynucleotides. *Nucleic Acids Research*. 2010;38(5):1623-35.

143. Jing N, Li Y, Xiong W, Sha W, Jing L, Tweardy DJ. G-quartet oligonucleotides: A new class of signal transducer and activator of transcription 3 inhibitors that suppresses growth of prostate and breast tumors through induction of apoptosis. *Cancer Research*. 2004;64(18):6603-9.

144. Li L, Cao JQ, Liu HM, Wu Q, Pan QH, Zeng ZP, et al. Microwave-assisted synthesis of imidazo[4,5-f][1,10]phenanthroline derivatives as apoptosis inducers in chemotherapy by stabilizing bcl-2 g-quadruplex DNA. *Molecules*. 2017;22(5):829-840.

145. Bates PJ, Kahlon JB, Thomas SD, Trent JO, Miller DM. Antiproliferative activity of g-rich oligonucleotides correlates with protein binding. *Journal of Biological Chemistry*. 1999;274(37):26369-77.

146. Bates PJ, Laber DA, Miller DM, Thomas SD, Trent JO. Discovery and development of the g-rich oligonucleotide as1411 as a novel treatment for cancer. *Experimental and Molecular Pathology*. 2009;86(3):151-64.

147. Girvan AC, Teng Y, Casson LK, Thomas SD, Juliger S, Ball MW, et al. Agro100 inhibits activation of nuclear factor-kappab (NF-kappab) by forming a complex with NF-kappab essential modulator (nemo) and nucleolin. *Molecular Cancer Therapeutics*. 2006;5(7):1790-9.

148. Hanakahi LA, Sun H, Maizels N. High affinity interactions of nucleolin with g-g-paired rdna. *Journal of Biological Chemistry*. 1999;274(22):15908-12.

149. Dempsey LA, Sun H, Hanakahi LA, Maizels N. G4 DNA binding by lr1 and its subunits, nucleolin and hnrnp d, a role for g-g pairing in immunoglobulin switch recombination. *Journal of Biological Chemistry*. 1999;274(2):1066-71.

150. Bugler B, Caizergues-Ferrer M, Bouche G, Bourbon H, Amalric F. Detection and localization of a class of proteins immunologically related to a 100-kDa nucleolar protein. *European Journal of Biochemistry*. 1982;128(2-3):475-80.

151. Ginisty H, Sicard H, Roger B, Bouvet P. Structure and functions of nucleolin. *Journal of Cell Science*. 1999;112 (Pt 6):761-72.

152. Abdelmohsen K, Gorospe M. Rna-binding protein nucleolin in disease. *RNA Biology*. 2012;9(6):799-808.

153. Tajrishi MM, Tuteja R, Tuteja N. Nucleolin: The most abundant multifunctional phosphoprotein of nucleolus. *Communicative & Integrative Biology*. 2011;4(3):267-75.

154. Cong R, Das S, Ugrinova I, Kumar S, Mongelard F, Wong J, et al. Interaction of nucleolin with ribosomal RNA genes and its role in RNA polymerase I transcription. *Nucleic Acids Research*. 2012;40(19):9441-54.

155. Durut N, Saez-Vasquez J. Nucleolin: Dual roles in rDNA chromatin transcription. *Gene*. 2015;556(1):7-12.

156. Ugrinova I, Monier K, Ivaldi C, Thiry M, Storck S, Mongelard F, et al. Inactivation of nucleolin leads to nucleolar disruption, cell cycle arrest and defects in centrosome duplication. *British Journal of Pharmacology*. 2007;8:66-82.

157. Storck S, Thiry M, Bouvet P. Conditional knockout of nucleolin in DT40 cells reveals the functional redundancy of its rna-binding domains. *Biology of the Cell*. 2009;101(3):153-67.

158. Wolfson E, Solomon S, Schmukler E, Goldshmit Y, Pinkas-Kramarski R. Nucleolin and erbb2 inhibition reduces tumorigenicity of erbb2-positive breast cancer. *Cell Death & Disease*. 2018;9(2):47-60.

159. Wolfson E, Goldenberg M, Solomon S, Frishberg A, Pinkas-Kramarski R. Nucleolin-binding by erbb2 enhances tumorigenicity of erbb2-positive breast cancer. *Oncotarget*. 2016;7(40):65320-34.

160. Xu X, Hamhouyia F, Thomas SD, Burke TJ, Girvan AC, McGregor WG, et al. Inhibition of DNA replication and induction of s phase cell cycle arrest by g-rich oligonucleotides. *Journal of Biological Chemistry*. 2001;276(46):43221-30.

161. Ireson CR, Kelland LR. Discovery and development of anticancer aptamers. *Molecular Cancer Therapeutics*. 2006;5(12):2957-62.

162. Soundararajan S, Chen W, Spicer EK, Courtenay-Luck N, Fernandes DJ. The nucleolin targeting aptamer as1411 destabilizes bcl-2 messenger RNA in human breast cancer cells. *Cancer Research*. 2008;68(7):2358-65.

163. Otake Y, Soundararajan S, Sengupta TK, Kio EA, Smith JC, Pineda-Roman M, et al. Overexpression of nucleolin in chronic lymphocytic leukemia cells induces stabilization of bcl2 mrna. *Blood*. 2007;109(7):3069-75.

164. Ishimaru D, Zuraw L, Ramalingam S, Sengupta TK, Bandyopadhyay S, Reuben A, et al. Mechanism of regulation of bcl-2 mRNA by nucleolin and a+u-rich element-binding factor 1 (AUF1). *Journal of Biological Chemistry*. 2010;285(35):27182-91.

165. Reyes-Reyes EM, Teng Y, Bates PJ. A new paradigm for aptamer therapeutic as1411 action: Uptake by macropinocytosis and its stimulation by a nucleolin-dependent mechanism. *Cancer Research*. 2010;70(21):8617-29.

166. Lim JP, Gleeson PA. Macropinocytosis: An endocytic pathway for internalising large gulps. *Immunology and Cell Biology*. 2011;89(8):836-43.

167. Schnelzer A, Prechtel D, Knaus U, Dehne K, Gerhard M, Graeff H, et al. Rac1 in human breast cancer: Overexpression, mutation analysis, and characterization of a new isoform, rac1b. *Oncogene*. 2000;19(26):3013-20.

168. Maltese WA, Overmeyer JH. Methuosis: Nonapoptotic cell death associated with vacuolization of macropinosome and endosome compartments. *The American Journal of Pathology*. 2014;184(6):1630-42.

169. Bhanot H, Young AM, Overmeyer JH, Maltese WA. Induction of nonapoptotic cell death by activated ras requires inverse regulation of rac1 and arf6. *Molecular Cancer Research*. 2010;8(10):1358-74.

170. Reyes-Reyes EM, Salipur FR, Shams M, Forsthoefel MK, Bates PJ. Mechanistic studies of anticancer aptamer as1411 reveal a novel role for nucleolin in regulating rac1 activation. *Molecular Oncology*. 2015;9(7):1392-405.

171. Nahar M, Dutta T, Murugesan S, Asthana A, Mishra D, Rajkumar V, et al. Functional polymeric nanoparticles: An efficient and promising tool for active delivery of bioactives. *Critical Reviews in Therapeutic Drug Carrier Systems*. 2006;23(4):259-318.

172. Bahrami B, Hojjat-Farsangi M, Mohammadi H, Anvari E, Ghalamfarsa G, Yousefi M, et al. Nanoparticles and targeted drug delivery in cancer therapy. *Immunology Letters*. 2017;190:64-83.

173. Singh R, Lillard JW, Jr. Nanoparticle-based targeted drug delivery. *Experimental and Molecular Pathology*. 2009;86(3):215-23.

174. Maeda H, Nakamura H, Fang J. The epr effect for macromolecular drug delivery to solid tumors: Improvement of tumor uptake, lowering of systemic toxicity, and distinct tumor imaging in vivo. *Advanced Drug Delivery Reviews*. 2013;65(1):71-9.

175. Liong M, Lu J, Kovochich M, Xia T, Ruehm SG, Nel AE, et al. Multifunctional inorganic nanoparticles for imaging, targeting, and drug delivery. *ACS Nano*. 2008;2(5):889-96.

176. Chapman S, Dobrovolskaia M, Farahani K, Goodwin A, Joshi A, Lee H, et al. Nanoparticles for cancer imaging: The good, the bad, and the promise. *Nano Today*. 2013;8(5):454-60.

177. Mamaeva V, Rosenholm JM, Bate-Eya LT, Bergman L, Peuhu E, Duchanoy A, et al. Mesoporous silica nanoparticles as drug delivery systems for targeted inhibition of notch signaling in cancer. *Molecular Therapy*. 2011;19(8):1538-46.

178. Farokhzad OC, Langer R. Impact of nanotechnology on drug delivery. *ACS Nano*. 2009;3(1):16-20.

179. De Jong WH, Borm PJ. Drug delivery and nanoparticles:Applications and hazards. *International Journal of Nanomedicine*. 2008;3(2):133-49.

180. Ji SR, Liu C, Zhang B, Yang F, Xu J, Long J, et al. Carbon nanotubes in cancer diagnosis and therapy. *Biochimica et Biophysica Acta*. 2010;1806(1):29-35.

181. Wang Y, Tu S, Pinchuk AN, Xiong MP. Active drug encapsulation and release kinetics from hydrogel-in-liposome nanoparticles. *Journal of Colloid and Interface Science*. 2013;406:247-55.

182. Zununi Vahed S, Salehi R, Davaran S, Sharifi S. Liposome-based drug co-delivery systems in cancer cells. *Materials Science and Engineering C: Materials for Biological Applications*. 2017;71:1327-41.

183. Sepantafar M, Maheronnaghsh R, Mohammadi H, Radmanesh F, Hasani-Sadrabadi MM, Ebrahimi M, et al. Engineered hydrogels in cancer therapy and diagnosis. *Trends in Biotechnology*. 2017;35(11):1074-87.

184. Prabhu RH, Patravale VB, Joshi MD. Polymeric nanoparticles for targeted treatment in oncology: Current insights. *International Journal of Nanomedicine*. 2015;10:1001-18.

185. Baker JR, Jr. Dendrimer-based nanoparticles for cancer therapy. *Hematology ASH Education Program*. 2009:708-19.

186. Biswas S, Kumari P, Lakhani PM, Ghosh B. Recent advances in polymeric micelles for anti-cancer drug delivery. *European Journal of Pharmaceutical Sciences*. 2016;83:184-202.

187. Slowing, II, Vivero-Escoto JL, Wu CW, Lin VS. Mesoporous silica nanoparticles as controlled release drug delivery and gene transfection carriers. *Advanced Drug Delivery Reviews*. 2008;60(11):1278-88.

188. Mekaru H, Lu J, Tamanoi F. Development of mesoporous silica-based nanoparticles with controlled release capability for cancer therapy. *Advanced Drug Delivery Reviews*. 2015;95:40-9.

189. He X, Zhao Y, He D, Wang K, Xu F, Tang J. ATP-responsive controlled release system using aptamer-functionalized mesoporous silica nanoparticles. *Langmuir*. 2012;28(35):12909-15.

190. Merisko-Liversidge EM, Liversidge GG. Drug nanoparticles: Formulating poorly water-soluble compounds. *Toxicologic Pathology*. 2008;36(1):43-8.

191. Kalepu S, Nekkanti V. Insoluble drug delivery strategies: Review of recent advances and business prospects. *Acta Pharmaceutica Sinica B*. 2015;5(5):442-53.

192. Natarajan JV, Nugraha C, Ng XW, Venkatraman S. Sustained-release from nanocarriers: A review. *Journal of Controlled Release*. 2014;193:122-38.

193. Kadam RS, Bourne DW, Kompella UB. Nano-advantage in enhanced drug delivery with biodegradable nanoparticles: Contribution of reduced clearance. *Drug Metabolism and Disposition*. 2012;40(7):1380-8.

194. Din FU, Aman W, Ullah I, Qureshi OS, Mustapha O, Shafique S, et al. Effective use of nanocarriers as drug delivery systems for the treatment of selected tumors. *International Journal of Nanomedicine*. 2017;12:7291-309.

195. Siegel RA, Rathbone MJ. Overview of controlled release mechanisms. In: Siepmann J, Siegel RA, Rathbone MJ, editors. Fundamentals and applications of controlled release drug delivery. Boston, MA: Springer US; 2012:19-43.

196. Lee JH, Yeo Y. Controlled drug release from pharmaceutical nanocarriers. *Chemical Engineering Science*. 2015;125:75-84.

197. Zhang X, Meng L, Lu Q, Fei Z, Dyson PJ. Targeted delivery and controlled release of doxorubicin to cancer cells using modified single wall carbon nanotubes. *Biomaterials*. 2009;30(30):6041-7.

198. Li H-F, Wu C, Xia M, Zhao H, Zhao M-X, Hou J, et al. Targeted and controlled drug delivery using a temperature and ultra-violet responsive liposome with excellent breast cancer suppressing ability. *RSC Advances*. 2015;5(35):27630-9.

199. Zhang W, Zhang Z, Zhang Y. The application of carbon nanotubes in target drug delivery systems for cancer therapies. *Nanoscale Research Letters*. 2011;6:555-77.

200. Liu Z, Chen K, Davis C, Sherlock S, Cao Q, Chen X, et al. Drug delivery with carbon nanotubes for in vivo cancer treatment. *Cancer Research*. 2008;68(16):6652-60.

201. Patlolla A, Knighten B, Tchounwou P. Multi-walled carbon nanotubes induce cytotoxicity, genotoxicity and apoptosis in normal human dermal fibroblast cells. *Ethnicity & Disease*. 2010;20(1 Suppl 1):S1-65-72.

202. Tian F, Cui D, Schwarz H, Estrada GG, Kobayashi H. Cytotoxicity of single-wall carbon nanotubes on human fibroblasts. *Toxicology in Vitro*. 2006;20(7):1202-12.

203. Geckeler KE, Premkumar T. Carbon nanotubes: Are they dispersed or dissolved in liquids? *Nanoscale Research Letters*. 2011;6(1):136-9.

204. Dutta RC. Drug carriers in pharmaceutical design: Promises and progress. *Current Pharmaceutical Design*. 2007;13(7):761-9.

205. Layek B, Mukherjee B. Tamoxifen citrate encapsulated sustained release liposomes: Preparation and evaluation of physicochemical properties. *Scientia Pharmaceutica*. 2010;78(3):507-15.

206. Selvam P, Bhatia SK, Sonwane CG. Recent advances in processing and characterization of periodic mesoporous MCM-41 silicate molecular sieves. *Industrial & Engineering Chemistry Research*. 2001;40(15):3237-61.

207. Vallet-Regi M, Balas F, Arcos D. Mesoporous materials for drug delivery. *Angewandte Chemie International Edition in English*. 2007;46(40):7548-58.

208. Kwon S, Singh RK, Perez RA, Abou Neel EA, Kim HW, Chrzanowski W. Silica-based mesoporous nanoparticles for controlled drug delivery. *Journal of Tissue Engineering*. 2013;4:2041731413503357.

209. Klichko Y, Liong M, Choi E, Angelos S, Nel AE, Stoddart JF, et al. Mesostructured silica for optical functionality, nanomachines, and drug delivery. *Journal of the American Ceramic Society*. 2009;92(s1):s2-s10.

210. Lu J, Liong M, Li Z, Zink JI, Tamanoi F. Biocompatibility, biodistribution, and drug-delivery efficiency of mesoporous silica nanoparticles for cancer therapy in animals. *Small*. 2010;6(16):1794-805.

211. Florek J, Caillard R, Kleitz F. Evaluation of mesoporous silica nanoparticles for oral drug delivery - current status and perspective of MSNs drug carriers. *Nanoscale*. 2017;9(40):15252-77.

212. Zhang J, Rosenholm JM. The viability of mesoporous silica nanoparticles for drug delivery. *Therapeutic Delivery*. 2015;6(8):891-3.

213. Koninti RK, Palvai S, Satpathi S, Basu S, Hazra P. Loading of an anti-cancer drug into mesoporous silica nano-channels and its subsequent release to DNA. *Nanoscale*. 2016;8(43):18436-45.

214. Slowing I, Trewyn BG, Lin VS. Effect of surface functionalization of mcm-41-type mesoporous silica nanoparticles on the endocytosis by human cancer cells. *Journal of the American Chemical Society*. 2006;128(46):14792-3.

215. Kwon IK, Lee SC, Han B, Park K. Analysis on the current status of targeted drug delivery to tumors. *Journal of Controlled Release*. 2012;164(2):108-14.

216. He D, He X, Wang K, Chen M, Cao J, Zhao Y. Reversible stimuli-responsive controlled release using mesoporous silica nanoparticles functionalized with a smart DNA molecule-gated switch. *Journal of Materials Chemistry*. 2012;22(29):14715-21.

217. Ozalp VC, Schafer T. Aptamer-based switchable nanovalves for stimuli-responsive drug delivery. *Chemistry*. 2011;17(36):9893-6.

218. Ozalp VC, Pedersen TR, Nielsen LJ, Olsen LF. Time-resolved measurements of intracellular atp in the yeast Saccharomyces Cerevisiae using a new type of nanobiosensor. *Journal of Biological Chemistry*. 2010;285(48):37579-88.

219. He D, He X, Wang K, Cao J, Zhao Y. A light-responsive reversible molecule-gated system using thymine-modified mesoporous silica nanoparticles. *Langmuir*. 2012;28(8):4003-8.

220. Zhang P, Kong J. Doxorubicin-tethered fluorescent silica nanoparticles for ph-responsive anticancer drug delivery. *Talanta*. 2015;134:501-7.

221. Zhao Z, Meng H, Wang N, Donovan MJ, Fu T, You M, et al. A controlled-release nanocarrier with extracellular ph value driven tumor targeting and translocation for drug delivery. *Angewandte Chemie International Edition in English*. 2013;52(29):7487-91.

222. Thomas CR, Ferris DP, Lee JH, Choi E, Cho MH, Kim ES, et al. Noninvasive remote-controlled release of drug molecules in vitro using magnetic actuation of mechanized nanoparticles. *Journal of the American Chemical Society*. 2010;132(31):10623-5.

223. Chen J, Liu M, Chen C, Gong H, Gao C. Synthesis and characterization of silica nanoparticles with well-defined thermoresponsive pnipam via a combination of raft and click chemistry. *ACS Applied Materials & Interfaces*. 2011;3(8):3215-23.

224. Yuan Q, Zhang Y, Chen T, Lu D, Zhao Z, Zhang X, et al. Photon-manipulated drug release from a mesoporous nanocontainer controlled by azobenzene-modified nucleic acid. *ACS Nano*. 2012;6(7):6337-44.

225. Wang W, Yan T, Cui S, Wan J. A bioresponsive controlled-release biosensor using au nanocages capped with an aptamer-based molecular gate and its application in living cells. *Chemical Communications*. 2012;48(82):10228-30.

226. Zhu CL, Lu CH, Song XY, Yang HH, Wang XR. Bioresponsive controlled release using mesoporous silica nanoparticles capped with aptamer-based molecular gate. *Journal of the American Chemical Society*. 2011;133(5):1278-81.

227. Hernandez FJ, Hernandez LI, Pinto A, Schafer T, Ozalp VC. Targeting cancer cells with controlled release nanocapsules based on a single aptamer. *Chemical Communications*. 2013;49(13):1285-7.

228. Ercan M. Genotyping a thalassemia point mutation by probe-gated silica nanoparticles. Istanbul, Turkey: Yeditepe University; 2017.

229. Ercan M, Ozalp VC, Tuna BG. Genotyping of single nucleotide polymorphism by probe-gated silica nanoparticles. *Analytical Biochemistry*. 2017;537:78-83.

230. Li J, Miao X, Hao Y, Zhao J, Sun X, Wang L. Synthesis, amino-functionalization of mesoporous silica and its adsorption of cr(vi). *Journal of Colloid and Interface Science*. 2008;318(2):309-14.

231. Lee BE, Choi BY, Hong DK, Kim JH, Lee SH, Kho AR, et al. The cancer chemotherapeutic agent paclitaxel (taxol) reduces hippocampal neurogenesis via down-regulation of vesicular zinc. *Scientific Reports*. 2017;7(1):11667-77.

232. Seidman AD. Single-agent use of taxol (paclitaxel) in breast cancer. *Annals of Oncology*. 1994;5 Suppl 6:S17-22.

233. Kornblith P, Wells A, Gabrin MJ, Piwowar J, George LD, Ochs RL, et al. Breast cancer--response rates to chemotherapeutic agents studied in vitro. *Anticancer Research*. 2003;23(4):3405-11.

234. Nemcova-Furstova V, Kopperova D, Balusikova K, Ehrlichova M, Brynychova V, Vaclavikova R, et al. Characterization of acquired paclitaxel resistance of breast cancer cells and involvement of abc transporters. *Toxicology and Applied Pharmacology*. 2016;310:215-28.

235. Biesuz R, Emma G, Milanese C, Dacarro G, Taglietti A, Nurchi VM, et al. Novel dfo-sam on mesoporous silica for iron sensing. Part I. Synthesis optimization and characterization of the material. *Analyst*. 2014;139(16):3932-9.

236. Orita T, Tomita M, Nakanishi K, Kato K. Immunoprecipitation of bisphenol a by antibody–mesoporous silica composites. *Journal of Asian Ceramic Societies*. 2014;2(3):275-80.

237. Al Samri MT, Biradar AV, Alsuwaidi AR, Balhaj G, Al-Hammadi S, Shehab S, et al. In vitro biocompatibility of calcined mesoporous silica particles and fetal blood cells. *International Journal of Nanomedicine*. 2012;7:3111-21.

APPENDIX A: ETHICAL APPROVAL FORM

YEDİTEPE ÜNİVERSİTESİ

T.C. YEDİTEPE ÜNİVERSİTESİ, DENEY HAYVANLARI ETİK KURULU (YÜDHEK)

ETİK KURUL KARARI

Toplantı Tarihi	Karar No	İlgi	Proje Yürütücüsü
25.07.2016	554	22.07.2016	Doç. Dr. Veli Cengiz Özalp

'Doxorubicin ilaç etkinliğinin aptamer kapılı silika nanokürelerin hedeflenme ve kontrollü salınımı yoluyla iyileştirilmesi' adlı bilimsel çalışma etik kurulumuzda görüşülmüş olup, çalışmanın etik kurallara uygun olduğuna oy birliğiyle karar verilmiştir.

Etik Onay Geçerlilik Süresi: 2 Yıl	**Hayvan Türü ve cinsiyeti:** Fare ♀	**Hayvan Sayısı:** 30

GÖREVİ	ADI SOYADI	İMZA
Başkan	Prof. Dr. M. Ece GENÇ	
Başkan Yardımcısı	Prof. Dr. Erdem YEŞİLADA	
Raportör	Prof. Dr. Işıl AKSAN KURNAZ	
Üye	Prof. Dr. Bayram YILMAZ	
Üye	Prof. Dr. Başar ATALAY	
Üye	Doç. Dr. Soner DOĞAN	KATILMADI
Üye	Doç. Dr. Ediz DENİZ	
Üye	Doç. Dr. C. Narter YEŞİLDAĞLAR	KATILMADI
Üye	Sumru KİRAZCI	